Morphology and phylogenetic relationships of a new eschrichtiid genus (Cetacea: Mysticeti) from the Early Pliocene of northern Italy

MICHELANGELO BISCONTI*

Dipartimento di Scienze della Terra, Università di Pisa, Via Santa Maria 53, 56126, Pisa, Italy

A new eschrichtiid, ***Eschrichtioides gastaldii*** **gen. nov., comb. nov.**, is established based on a specimen previously assigned to *Balaenoptera gastaldii* Portis, 1885. The holotype is from the Early Pliocene of north-east Italy. It represents a fossil mysticete closely related to the living grey whale, *Eschrichtius robustus*. Comparative morphology and phylogenetic analysis support the monophyly of Eschrichtiidae and *Cetotherium*-like mysticetes and a sister group relationship between this clade and Balaenopteridae. Eschrichtiid fossils previously described are all from the Pleistocene and Late Pliocene while *Eschrichtioides gastaldii* is from the Early Pliocene. The recognition of this new eschrichtiid genus suggests that the Mediterranean trophic web of the Early Pliocene was more complex than at present and that the Neogene mysticete family-level biodiversity of the Mediterranean was higher than that currently observed in this basin.   © 2008 The Linnean Society of London, *Zoological Journal of the Linnean Society*, 2008, **153**, 161–186.

ADDITIONAL KEYWORDS: Eschrichtiidae – *Eschrichtioides gastaldii* – *Eschrichtius robustus* – feeding adaptations – grey whale.

INTRODUCTION

In his monumental work published in 1885, Alessandro Portis described many cetacean remains from north-west Italy, many of which are now housed in the Museo Regionale di Scienze Naturali, Torino (Regional Natural History Museum, Turin). He detailed the discoveries of cetacean fossils found in Italy since the early 19th century, providing a historical reconstruction fundamental to our understanding of the complex synonymy of the Italian record of this group. He also provided photographic plates illustrating some of the most debated mysticete fossils of the Italian Pliocene. One of them is his '*Balaenoptera*' *gastaldii* Portis, 1885 consisting of a fairly well-preserved skull, dentaries and some postcranial elements. This specimen was found by Cortesi in 1816 near the town of Cortandone, a few kilometres from Asti, and was studied by Brandt (1873) who assigned

it to *Cetotherium gastaldii*. Just two years later, Van Beneden (1875) included it within *Plesiocetus cortesii* together with approximately all the other non-balaenid mysticete remains found in the Italian Pliocene. Portis (1885) assigned the specimen to *Balaenoptera*, and Sacco (1890) suggested that it belonged to a subspecies of *Plesiocetus cortesii*, namely *P. cortesii gastaldii*. Finally, Caretto (1970) included the specimen within the chronospecies *Balaenoptera acutorostrata cuvieri* whose status has been criticized by Deméré & Berta (2003) and Bisconti (2003a).

After a careful examination of its skull morphology, it is clear to me that the specimen from Cortandone represents a new genus of an eschrichtiid mysticete. The specimen has been included in phylogenetic analyses performed by Bisconti (2003a) and Deméré, Berta & McGowen (2005), resulting in its inclusion in the family Eschrichtiidae. Today, the family Eschrichtiidae is monotypic being represented only by the grey whale *Eschrichtius robustus* Lilljeborg, 1861. In their analysis of the evolutionary history of the grey whale,

*E-mail: bisconti@dst.unipi.it

Barnes & McLeod (1984) listed some fossil and subfossil materials pertaining to the species. More recently, the description of an incomplete, juvenile individual assigned to *Eschrichtius* sp. from the Yuchi Formation of Japan has extended the fossil record of Eschrichtiidae back to the Late Pliocene (Ichishima *et al.*, 2006). Bisconti & Varola (2006) augmented the records by the description of *Archaeschrichtius ruggieroi* Bisconti & Varola, 2006, a fragmentary dentary assigned to Eschrichtiidae, which is from the Late Miocene of the Mediterranean Basin. The discovery of a new eschrichtiid in the Pliocene of the Mediterranean Basin adds new important information about the past diversity of the family and helps in the reconstruction of the phylogenetic relationships of the living grey whale.

The new genus shares morphological traits with both Eschrichtiidae and Cetotheriidae *sensu* Bouetel & de Muizon (2006; hereafter, I include in the family Cetotheriidae the following *Cetotherium*-like mysticetes: *Cetotherium rathkei* Brandt, 1843, *Mixocetus elysius* Kellogg, 1934 and *Metopocetus durinasus* Cope, 1896. Moreover, the dentary of the new taxon shares a number of apomorphic features with *Eschrichtius robustus* suggesting that both used similar filter-feeding mechanisms.

In this paper, the new genus is described and compared, and its phylogenetic relationships are investigated through a morphology-based cladistic analysis using 165 characters scored for 35 taxa. The results of this work form part of a larger project of study and revision of the Italian mysticete fossils ongoing since 1995 and that has already resulted in a series of published papers (Bisconti, 2000, 2002, 2003b, 2006; Bisconti & Varola, 2000, 2006).

Anatomical abbreviations: ap, angular process of dentary; apmx, ascending process of maxilla; atc, ascending temporal crest; bcf, basicapsular fissure; boc, basioccipital; cp, coronoid process of dentary; dpb, descending process of basioccipital; dpc, deltopectoral crest; eam, external acoustic meatus; exoc, exoccipital; fm, foramen magnum; fpo, foramen 'pseudo-ovale'; gcs, groove between coronoid and satellite process; gml, groove for mental ligament; gvb, groove for vasculature of the baleen; hh, humeral head; ip, interparietal; irfr, interorbital region of frontal; mdc, mandibular condyle; mf, mandibular foramen; mhg, mylohyoidal groove; mx, maxilla; mxf, maxillary foramina; n, nasal; nf, narial fossa; o, orbit; oc, occipital condyle; op, olecranon process; p, parietal; pal, palatine; pmx, premaxilla; pt, pterygoid; soc, supraoccipital; sop, supraorbital process of frontal; sp., satellite process of dentary; s P-F, suture between parietal and frontal; sq, squamosal; ts, tubercle on the surface of the supraoccipital; V, vomer; zps, zygomatic process of squamosal.

Institutional abbreviations: ChM, The Charleston Museum, Charleston, USA; IRSN, Institut Royal des Sciences Naturelles, Brussels, Belgium; MGB, Museo Geopalaeontologico 'G. Capellini', Bologna, Italy; MCA, Museo Geopalaeontologico 'G. Cortesi', Castell'Arquato, Italy; MRSN, Museo Regionale di Scienze Naturali, Torino, Italy; MSNT, Museo di Storia Naturale del Territorio, Calci, Italy; MPST, Museo Palaeontologico, Salsomaggiore Terme, Italy; NMB, NatuurMuseum Brabant, Tilburg, Holland; SMSN, Staatliches Museum für Naturkunde, Stuttgart, Germany; USNM, United States National Museum of Natural History, Smithsonian Institution, Washington, DC, USA; ZMA, Instituut voor Systematiek en Populatiebiologie/Zoölogisch Museum, Amsterdam, Holland; ZML, Zoölogisch Museum, Leiden, Holland.

SYSTEMATIC PALAEONTOLOGY
CLASS MAMMALIA LINNAEUS, 1758
SUPERORDER CETARTIODACTYLA MONTGELARD, CATZEFLIS, DOUZERY, 1997
ORDER CETACEA BRISSON, 1762
SUBORDER MYSTICETI FLOWER, 1864
FAMILY ESCHRICHTIIDAE ELLERMAN & MORRISON-SCOTT, 1951
***ESCHRICHTIOIDES* GEN. NOV.**

Diagnosis: Eschrichtioides differs from *Eschrichtius* in having a laterally bowed dentary, higher coronoid process of the dentary, straight rostrum in lateral view, smaller nasal and narrower interorbital constriction. It differs from *Archaeschrichtius* in having a rounded and lower satellite process and less dorsally located groove for the mental ligament.

Discussion: Eschrichtioides shares with the living *Eschrichtius robustus* the presence of a bilateral tubercle on the dorsolateral surface of the supraoccipital, ascending temporal crest abruptly projecting toward postorbital corner on supraorbital process of frontal, relatively anteroposteriorly short and steeply sloping supraoccipital, massive and short zygomatic process of the squamosal, robust and posteriorly directed paroccipital process, lateral wall of skull bulging into temporal fossa, several large foramina scattered on the maxilla lateral to the narial opening, condyle of dentary located dorsally, high angular process of dentary, dorsoventral arc of dentary, very low coronoid process, presence of mylohyoidal concavity on the medial side of the dentary. *Eschrichtioides* shares with *Archaeschrichtius* the presence of a satellite process in the dentary that is separated from

the coronoid process by a groove; the satellite process of *Archaeschrichtius* is higher, triangular and has a pointed apex.

Etimology: Eschrichtius, grey whale; *Eschrichtioides*, Latin, similar to *Eschrichtius*.

ESCHRICHTIOIDES GASTALDII COMB. NOV.

Cetotherium cortesii – Brandt, 1873: pls 21, 22; p. 153.
Cetotherium gastaldii: Strobel, 1875: p. 8.
Plesiocetus cortesii: Van Beneden, 1875; p. 755, 756
Cetotherium gastaldii: Strobel, 1881: pls 1, 2, 5; p. 13.
Balaenoptera gastaldii: Portis, 1883: p. 20.
Balaenoptera gastaldii: Portis, 1885: pls 1, 2; p. 17.
Balaenoptera acutorostrata: Caretto, 1970: p. 57.
'*Balaenoptera*' *gastaldii*: Deméré *et al.*, 2005: p. 105, 119

Holotype: MRSN 13802 including skull, right dentary (13802/3), left dentary (13802/4 PU), atlas (13802/8), axis (13802/6), fourth cervical vertebra (13802/7), a lumbar vertebra (13802/18), four caudal vertebrae (13802/9, 10, 11, 12), hyoid (13802/24), ulna, and two ribs of the left side. Portis (1885) listed also humerus, three metacarpals and four phalanxes, left jugal and a tympanic bulla but I was unable to find these specimens in the MRSN collection. Cranial measurements are provided in Table l.

Type locality: Cortandone (geographical coordinates of the town: 44°58′N, 18°27′E), a town located around 20 km WNW from Asti and around 5 km NE from Villafranca d'Asti in Piedmont (north-west Italy; Fig. 1).

Table 1. *Eschrichtioides gastaldii* **gen. nov., comb. nov.**, holotype. Cranial measurements in mm

Condylobasal length	930
Maximum width of skull (at anterior tip of zygomatic processes of squamosals)	490
Maximum transverse diameter of supraorbital process of frontal	160
Supraoccipital length	
Transverse diameter of foramen magnum	55
Dorsoventral diameter of foramen magnum	65
Posterior width of vomer	120
Length of right basicapsular fissure	120
Width of right basicapsular fissure	65
Length of left basicapsular fissure	105
Width of left basicapsular fissure	50
Length of right palatine	270
Width of right palatine	78
Length of left palatine	260
Width of left palatine	70

Formation and age: Sabbie d'Asti Formation. The Sabbie d'Asti Formation (Asti Sands Fm.) is developed at the top of the Argille Azzurre Formation (Blue Clays Fm.) (Ferrero & Pavia, 1996). Foraminifers sampled at the top of the Argille Azzurre Formation suggested that deposition of this formation ended during the latest Early Pliocene. The Sabbie d'Asti Formation is characterized by a high density of mollusc shells whose occurrence in the Mediterranean Basin has been constrained within a range of a few million years between the start of the Pliocene (5.3 Ma) and 3.0 Ma by studies of Raffi and co-workers (Raffi, Stanley & Marasti, 1985; Monegatti & Raffi, 2001). Interpretation of mollusc occurrence and extinction in the Sabbie d'Asti Formation by Ferrero & Pavia (1996, and references therein) suggests that the age of this formation can be con-
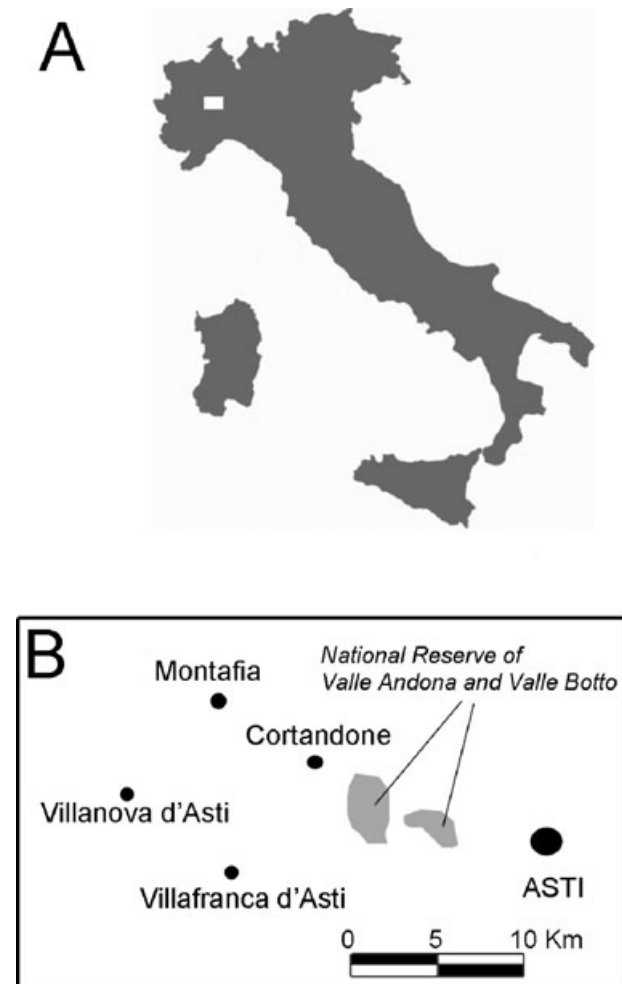

Figure 1. Discovery area of *Eschrichtioides gastaldii*. A, Italian peninsula; white rectangle represents the Cortandone area. B, Cortandone area.
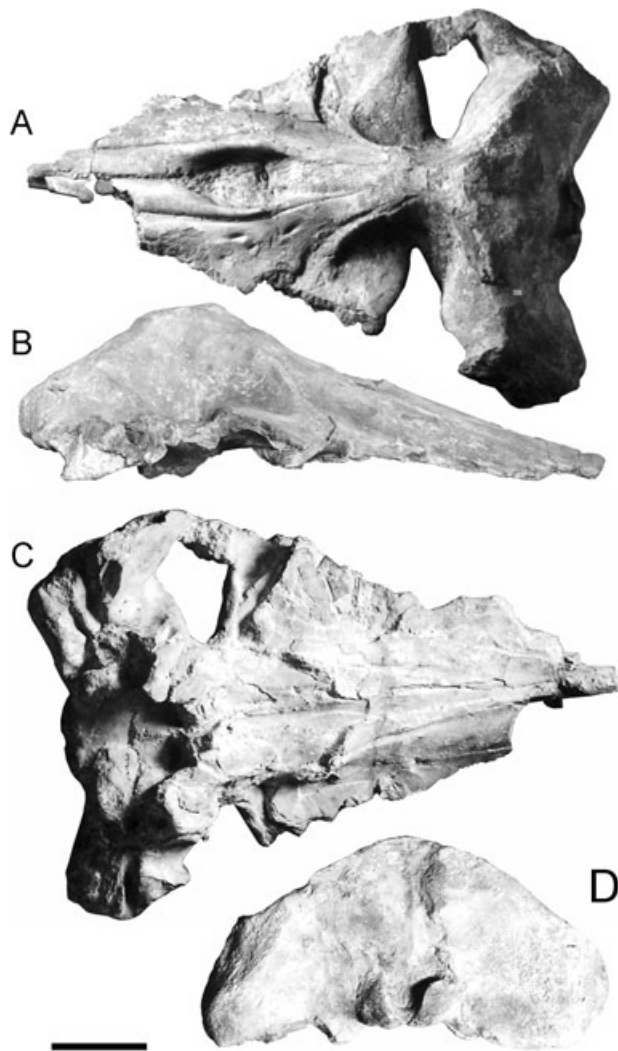
Figure 2. *Eschrichtioides gastaldii* **gen. nov., comb. nov.**: skull. A, dorsal view. B, right lateral view. C, ventral view. D, posterior view. Scale bar = 20 cm.

strained between late Zanclean and early Piacenzian but it is impossible to get a more precise chronostratigraphic assessment.

Diagnosis: As for the genus.

Etymology: The patronymic *gastaldii* was given by Strobel to the holotype specimen in recognition of the importance of the palaeontological work of Bartolomeo Gastaldi (Torino, 1818–1879).

DESCRIPTION

Skull
Premaxilla: Most of the anterior portion of the rostrum is lost (Figs 2, 3). The posterior end of the

premaxilla is located under the posteromedial corner of the maxilla, which is prolonged posteriorly to cover part of the interorbital region of the frontal. The premaxilla is medially concave anterior to the nasal bones on the side of the narial fossa; anterior to the narial fossa, the medial sides of the premaxillae converge toward the longitudinal axis of the skull and project anteriorly. There are no premaxillary foramina.

Maxilla: Maxilla horizontal and flat (Figs 2, 3). Lateral borders of the maxillae not preserved and this prevents an assessment of the whole width of the rostrum. Four maxillary foramina are present in the posterior and medial portion of the left maxilla lateral to the narial fossa. Posteromedial corner of the maxilla projecting posteriorly and superimposing onto the posterior end of the premaxilla and the interorbital region of the frontal, forming a long and narrow ascending process (Fig. 4). Posterior end of the ascending process rounded; its medial and lateral borders are parallel for their main development; more anterior portion of the ascending process of the maxilla wide, differing from balaenopterids in which this portion is narrower. In fact, this condition is closer to that of *Cetotherium*-like mysticetes. In ventral view, the surface of the maxilla bears only a few grooves for the vasculature of the baleen; among them, two grooves run parallel to the longitudinal axis of the skull very close to the mid-line; a groove is evident in the left maxillary which starts from a hole in the ventral surface of the bone and runs anteriorly. The medial portion of the maxilla gently protrudes ventrally, forming a longitudinal keel which is transversely wide and round. Infraorbital plate with a sharp posterior border directed anterolaterally; this condition is common among the mysticetes, being shared with *Eschrichtius robustus* and other mysticetes such as *Cophocetus oregonensis* Packard & Kellogg, 1934, *Aglaocetus moreni* Kellogg, 1934, *Pelocetus calvertensis* Kellogg, 1965 and *Diorocetus hiatus* Kellogg, 1968. Posterior border of the maxilla profoundly indented by the interposition of the palatine.

Nasal: Nasal long; dorsal surface flat; anterior border straight (Figs 2, 3). Anterior end of the nasal located on a transverse line crossing the anterior border of the supraorbital process of frontal; in *Parietobalaena palmeri* Kellogg, 1924, *Diorocetus hiatus*, *Pelocetus calvertensis*, *Aglaocetus moreni*, *Cophocetus oregonensis* and *Mixocetus elysius* the anterior end of the nasals is anterior to the anterior border of the supraorbital process of the frontal; in *Balaenoptera acutorostrata* Lacépède, 1804, *B. edeni* Anderson, 1878 and *B. borealis* Lesson, 1828 the anterior border of the nasals is slightly anterior to the anterior border
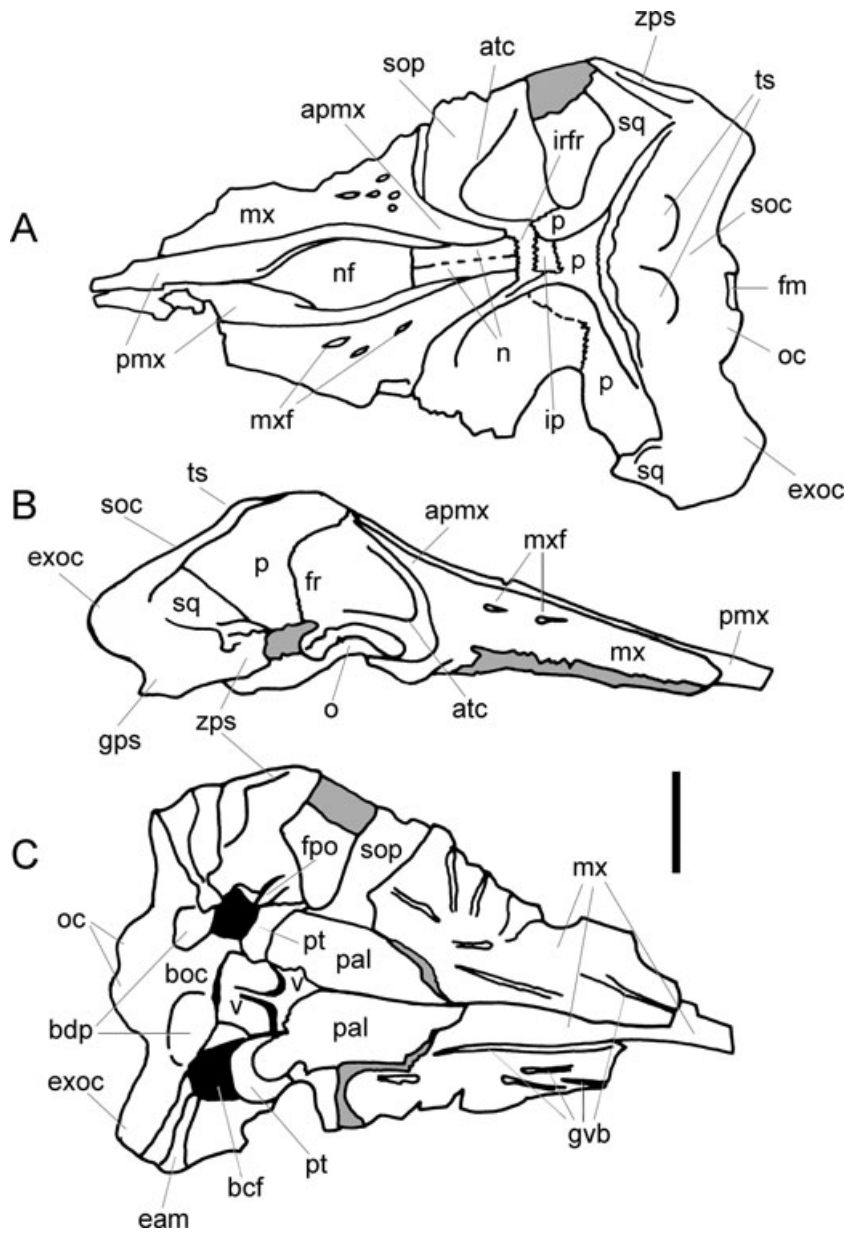
Figure 3. *Eschrichtioides gastaldii* **gen. nov., comb. nov.**: skull. A, dorsal view. B, right lateral view. C, ventral view. See Anatomical abbreviations for explanation of lettering. Scale bar = 20 cm.

of the supraorbital process of the frontal; in *Balaenoptera physalus* (Linnaeus, 1758) and *B. musculus* (Linnaeus, 1758) the anterior border is posterior to the anterior border of the supraorbital process of the frontal. Nasofrontal suture located on a transverse line crossing the middle of the orbit; suture slightly indented. The position of the nasofrontal suture is similar in *Cophocetus oregonensis*, *Aglaocetus moreni*, *Pelocetus calvertensis* and in living balaenopterids. In *Parietobalaena palmeri*, *Diorocetus hiatus* and *Aglaocetus patulus* the nasofrontal suture is located more anteriorly, near the anterior border of the interorbital

region of the frontal. Nasal and premaxilla contacting anteriorly; nasal and ascending process of maxilla contacting along the posterior half of nasal, the premaxilla being located beneath the maxilla in that region. This condition can be observed in specimens of *Megaptera novaeangliae* (Borowski, 1781) as illustrated by True (1904).

Frontal: Supraorbital process of the frontal abruptly depressed from the interorbital region as in eschrichtiids and balaenopterids (Figs 2, 3). Supraorbital process dorsally flat and crossed by an ascending
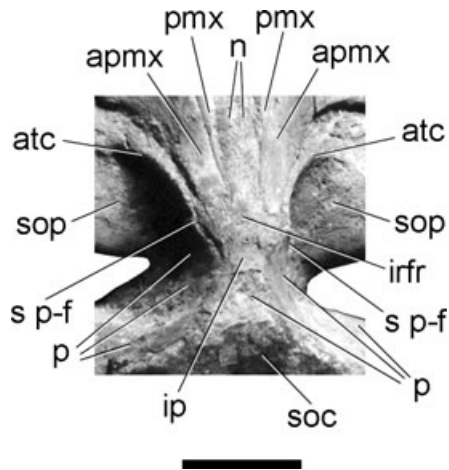
Figure 4. *Eschrichtioides gastaldii* gen. nov., comb. nov.: vertex. See Anatomical abbreviations for explanation of lettering. Scale bar = 5 cm.

temporal crest whose medial portion projects medially, and whose lateral portion abruptly projects posterolaterally towards the postorbital corner of the process in the proximity of the orbit. Interorbital region of the frontal almost completely hidden by the posteromedial elements of the rostrum: only a subtle sheet of bone is observed, which is located lateral and posterior to the ascending process of the maxilla, resembling the condition found in *Cetotherium*-like mysticetes. In ventral view, the channel for the optic nerve is highly concave and is surrounded by anterior and posterior crests, which are located under the central body of the supraorbital process of the frontal.

Parietal: In dorsal view, a strong postorbital constriction is observed posterior to the skull vertex (Figs 2, 3). The parietals appear dorsally anterior to the anterior border of the supraoccipital where their dorsolateral borders form short lateral concavities corresponding to the attachment sites for the temporalis muscle. In lateral view, anterior border of the parietal located more anteriorly than the posteriormost portion of the interorbital region of the frontal. Parietal not interdigitating with the posteromedial corner of the maxilla as in balaenopterids.

Squamosal: Only the right squamosal is sufficiently complete to allow a description of almost every feature of the bone (Figs 2, 3). Zygomatic process of the squamosal short and triangular in lateral view; it descends from the posterior apex of the lambdoidal crest with a steep inclination and terminates anterior to the anterior border of the supraoccipital. Posterior portion of the zygomatic process projecting anteriorly and laterally; anterior portion projecting only anteri-

orly, paralleling the longitudinal axis of the skull. Medial to the zygomatic process there is a broad, shallow, sharp squamosal fossa running along the dorsoventral axis; I observed such a fossa in all the specimens of *Eschrichtius robustus* that I have examined (Appendix 1) and in some specimens of *Balaenoptera borealis*. However, although all the examined eschrichtiids have this fossa, only a few specimens of *B. borealis* display the character, suggesting that this formation is highly variable in this balaenopterid species. The squamosal forms the posteromedial wall of the temporal fossa together with the parietal; both bones bulge into the fossa forming a globular expansion that must have included the brain hemispheres. The dorsal edge of the squamosal forms the posterior portion of the lambdoidal crest, which is rounded and whose posterior apex is triangular in dorsal view and is located on a transverse line anterior to the occipital condyles. In other mysticetes this formation may be shaped differently: in living balaenopterids, for instance, the posterior apex of the lambdoidal crest is triangular and anterior to the occipital condyles; in cetotheriids such as *Cophocetus oregonensis*, *Aglaocetus moreni*, *Mixocetus elysius* and *Pelocetus calvertensis* the posterior apex of the lambdoidal crest is nearly triangular and is located largely posterior to the occipital condyles; in other cetotheriids (such as *Parietobalaena palmeri*, *Diorocetus hiatus*, *Aglaocetus patulus* and *Piscobalaena nana* Pilleri & Siber, 1989) the posterior apex of the lambdoidal crest is wider and is located barely posterior or at the level of the occipital condyles.

Supraoccipital and exoccipital: The supraoccipital is short and wide; its main width is reached immediately dorsal to the foramen magnum; its anterior border is wide and round. In lateral view, the anterior portion of the supraoccipital is high and forms a sort of dome similar to that observed in the genus *Eubalaena* Gray, 1864 (Bisconti, 2002) and in *Eschrichtius robustus* (True, 1904) (Figs 2, 3). The dorsal surface of the supraoccipital bears a pair of tubercles located near the anterior border and in a parasagittal position; these tubercles are separated by a low sagittal ridge originating a few centimetres dorsal to the foramen magnum. The exoccipital projects posteriorly and laterally and its posterolateral corner is located at a considerable distance from the postglenoid process of the squamosal. This condition is shared with *Eschrichtius robustus*, *Piscobalaena nana*, *Metopocetus durinasus*, *Mixocetus elysius*, *Aglaocetus moreni* and *Titanocetus sammarinensis* Bisconti, 2006. In *Cophocetus oregonensis* the exoccipital protrudes posteriorly very markedly but the posterolateral corner is located more medially. In living balaenopterids the exoccipital does not protrude

posteriorly and its posterolateral corner is located much more medially than the postglenoid process. The occipital condyles are nearly flat. The dorsal border of each condyle is transversely wider than the ventral border. The foramen magnum is small and has linear dorsal and ventral borders.

Jugal: The anterior portion of the right jugal is small and projects anteriorly and ventrally (Fig. 5); at the

anteriormost end it protrudes medially. The posterior portion is dorsoventrally broader and flat. At mid length, a triangular projection protrudes distinctly dorsally.

Basicranium

Posterior to the maxilla, the palatine is broadly rectangular and has a posterior portion projecting posteriorly and laterally (Fig. 6). However, the posterior border of the palatine is not well preserved and it is not possible to assess the true morphology. The palatines are divided along the longitudinal axis by the interposition of the vomer. The posterolateral corner of the palatine is partially superimposed on the ventral surface of the pterygoid whose hamular process is transversely orientated and forms a ventral lamina corresponding to that described by Fraser & Purves (1960) in Balaenidae but developed to a lesser extent. As far as I am aware, a ventral lamina is present only in Balaenidae and Neobalaenidae. The pterygoid projects markedly ventrally and posteriorly. The vomer is interposed between the two pterygoids and is superimposed on the suture between the basioccipital and basisphenoid. The basioccipital is transversely short and bears two large and stocky
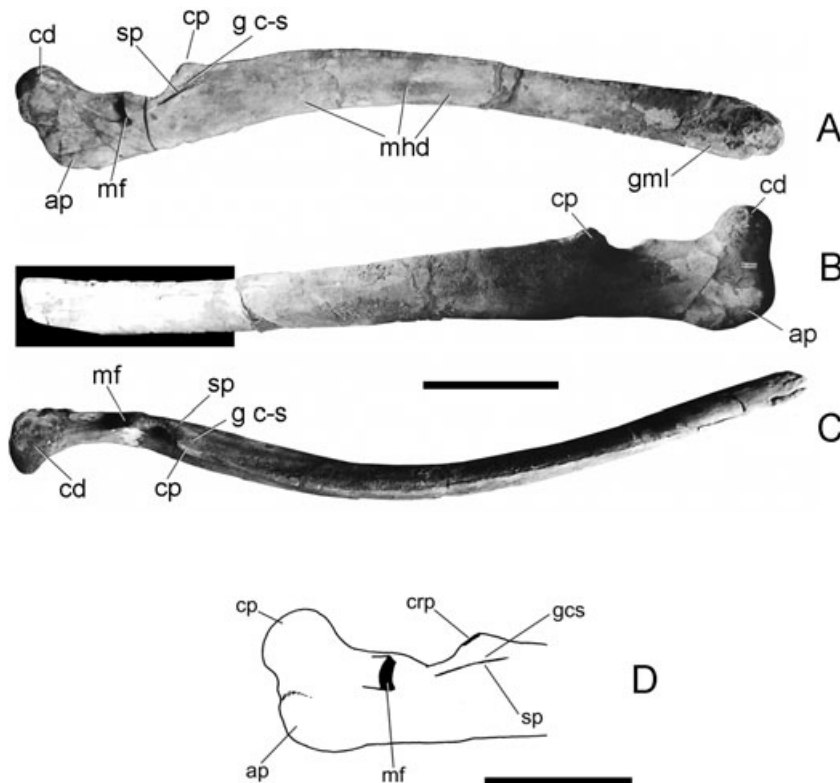

Figure 5. *Eschrichtioides gastaldii* **gen. nov., comb. nov.**: right jugal. Scale bar = 100 mm.

Figure 6. *Eschrichtioides gastaldii* **gen. nov., comb. nov.**. A, left dentary, medial view. B, left dentary, lateral view. C, right dentary, dorsal view. D, close-up of the left dentary showing the condyle and coronoid region in medial view. Scale bar = 15 cm in A, B and C, and 5 cm in D.

descending processes forming the posteromedial angle of the basicapsular fissure. The latter is not well preserved and is still partially filled with the matrix. The pars cochlearis of the right periotic is embedded in the matrix and its preservation is so poor that it cannot be fully described. The posterior process of the periotic appears as a strong crest between the postglenoid process of the squamosal and the posteroventral portion of the exoccipital. The exoccipital projects posteriorly and laterally as described above; it appears as a strong structure similar to that observed in *Cetotherium*-like mysticetes and *Eschrichtius robustus*.

I was unable to find the tympanic bulla in the MRSN collections. Portis (1885: pl. 2) showed a tympanic bulla associated with the skeleton of *E. gastaldii* which was transversely broad and anteroposteriorly short, resembling very closely the tympanic bulla of living eschrichtiids (see, for example, specimens USNM 364973, 504305 and 571931). The tympanic bulla of *Eschrichtius robustus* and *Eschrichtioides gastaldii* differs from that of living balaenopterids in that it is dorsoventrally higher and anteroposteriorly shorter; the bulla of these eschrichtiids is more compressed in both the anteroposterior and the dorsoventral axes.

Dentary
Measurements of the dentary are presented in Table 2. The dentary displays a continuous outward curvature that is interrupted at the level of the coronoid region; the neck of the bone is straight; the

Table 2. *Eschrichtioides gastaldii* **gen. nov., comb. nov.**, holotype. Measurements of the left dentary in mm

Length (straight)	1120
Length (curve)	1140
Height at anterior end	170
Height at condyle	90
Heigth at coronoid process	140
Minimum height between condyle and coronoid process	140
Height 100 mm behind anterior end	90
Height 200 mm behind anterior end	85
Height 300 mm behind anterior end	85
Height 400 mm behind anterior end	90
Height 500 mm behind anterior end	90
Height 600 mm behind anterior end	95
Height 700 mm behind anterior end	110
Height 800 mm behind anterior end	130
Height 900 mm behind anterior end	95
Height 1000 mm behind anterior end	160
Distance between condyle and coronoid process	200
Distance between coronoid process and anterior end	900

mandibular body exhibits a dorsoventral arc (Fig. 6). Anteriorly, the dentary does not show any sign of torsion and the groove for the mental ligament is only slightly developed; the dentary terminates anteriorly with a rounded border. Along the ventromedial surface of the ramus, a broad, shallow groove is observed which is located at a position consistent with the attachment of the mylohyoideus muscle; this groove is therefore considered homologous to the mylohyoidal sulcus of Balaenidae. Such a groove is absent in cetotheres and in balaenopterids; in the neobalaenid *Caperea marginata* Gray, 1873 the mylohyoidaeus muscle is attached to a medial depression rather than a groove as in Balaenidae.

The angular process of the dentary is robust, squared, and high and does not bear any groove for the attachment of pterygoideus muscles. The mandibular condyle is placed at the extremity of a posterodorsal projection, which brings it to a higher level than the top of the coronoid process; its articular surface is mainly orientated dorsally.

The coronoid region is quite complex. In lateral view, the coronoid process is a small and round emergence that is slightly higher than the dorsal border of the ramus; posteriorly, it continues into a postcoronoid crest whose lateral surface forms a wide, long postcoronoid fossa; immediately posterior to the postcoronoid crest, a round, shallow, long concavity is observed in the dorsal border of the dentary. In medial view, posterior to that concavity, there is the opening of a circular, small mandibular foramen which is prolonged into a broad groove projecting posteriorly and dorsally. The coronoid process is paralleled by a medial crest-like emergence which is separated from the coronoid process by a shallow, wide groove. This emergence is homologous to the satellite process described by Bisconti & Varola (2000, 2006) and it is found also in the living *Eschrichtius robustus*. Bisconti & Varola (2006) suggest that it represents a synapomorphy of Eschrichtiidae.

In cross-section, the anterior portion of the dentary has a convex surface both laterally and medially; the medial surface becomes nearly flat around 800 mm behind the anterior apex and shows a medial concavity about 880 mm behind the anterior apex (Fig. 7). The coronoid process and the parallel satellite process are evident in the section traced 900 mm behind the apex. Approaching the posterior end, the two sides become strongly convex.

Postcrania
Atlas: The atlas is largely broken. The articular surfaces with the occipital condyles are mainly concave (Fig. 8A); they are elongate dorsoventrally and narrow transversely. The neural channel is wider dorsally than ventrally. The articular surface for the
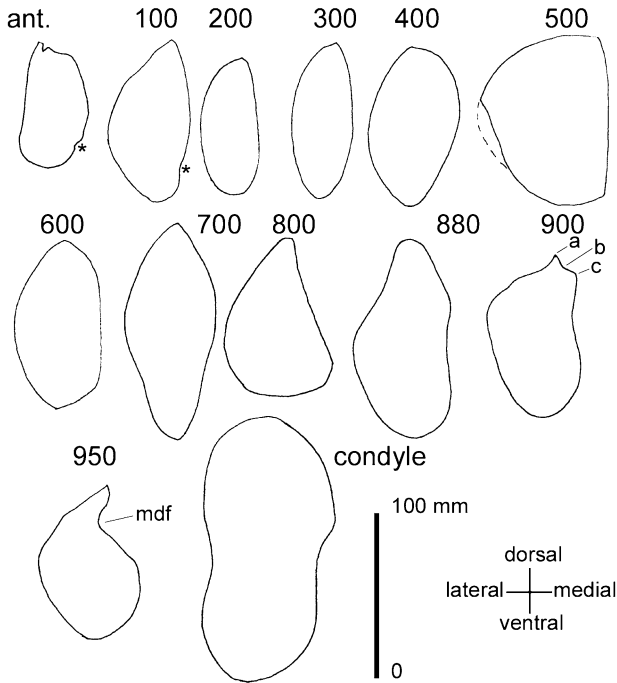
Figure 7. *Eschrichtioides gastaldii* **gen. nov., comb. nov.**: cross-sections of dentary. Selected cross-sections of the left dentary. Numbers over the sections are mm from the anterior end of the dentary. Scale bar = 100 mm. Explanation of abbreviations: a, coronoid process; b, groove between coronoid and satellite process; c, satellite process; mdf, mandibular foramen; *, groove for mental ligament. Broken line indicates missing portion of dentary.

axis is broadly convex. In lateral view, the atlas bears a foramen at the base of the broken dorsal transverse process lateral to the low neural arch. However, the height of the neural process cannot be estimated because it is broken at its base (measurements of postcranial bones are listed in Table 2).

Axis: The axis is almost complete (Fig. 8B). The articular surface with the atlas is concave laterally and convex medially; the border of the articular surface forms a heart-like figure. Ventrally, two massive processes develop which form the ventral border of the foramen transversarium; the distal end of the right process is wide and flat (this process is broken in the left process). The dorsal transverse process is more delicate and its distal end is broken on both sides. Judging from the preservation of the right ventral process, it seems that the foramen transversarium was not completely bordered by bone and that it was laterally incomplete. The neural arch is nearly triangular and is dorsally bordered by a strong, acute neural process which is developed just for a few centimetres due to a breakage of its apical end. The lateral surfaces of the neural arch descend gently laterally and ventrally.

Fourth cervical vertebra: This is largely incomplete, lacking neural arch and ventral transverse processes. The vertebra is tiny, delicate and short. The border of the articular surface is nearly quadrangular.
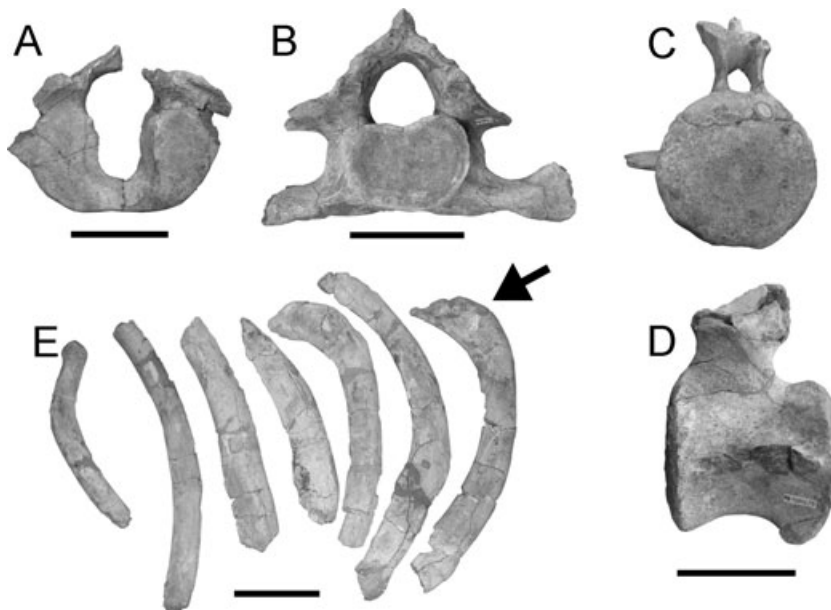

Figure 8. *Eschrichtioides gastaldii* **gen. nov., comb. nov.**: postcrania. A, atlas (rostral view). B, axis (caudal view). C, lumbar vertebra (rostral view). D, caudal vertebra (lateral view). E, ribs of the right side (note double-headed rib shown by arrowhead). Scale bars = 100 mm.

Table 3. *Eschrichtioides gastaldii* **gen. nov.**, comb. nov., holotype. Vertebral measurements in mm

Width of atlas (MGPT 13802/8)	170
Height of atlas	140
Length of atlas	35
Maximum diameter of neural channel of atlas	23
Width of axis (MGPT 13802/6)	265
Height of axis	165
Length of axis	38
Maximum dorsoventral diameter of neural channel of axis	75
Maximum transverse diameter of neural channel of axis	54
Width of centrum of vertebra MGPT 13802/7 (cervical)	90
Height of centrum of vertebra MGPT 13802/7 (cervical)	75
Length of centrum of vertebra MGPT 13802/7 (cervical)	21
Width of centrum of vertebra MGPT 13802/18 (lumbar)	105
Height of centrum of vertebra MGPT 13802/18 (lumbar)	85
Length of centrum of vertebra MGPT 13802/18 (lumbar)	105
Maximum with of vertebra MGPT 13802/18 (lumbar), including transverse process	135
Width of centrum of vertebra MGPT 13802/9 (caudal)	125
Height of centrum of vertebra MGPT 13802/9 (caudal)	120
Length of centrum of vertebra MGPT 13802/9 (caudal)	118
Total height of vertebra MGPT 13802/9 (caudal)	160
Maximum dorsoventral diameter of neural channel of 13802/9	35
Maximum transverse diameter of neural channel of 13802/9	23
Width of centrum of vertebra MGPT 13802/10 (caudal)	111
Height of centrum of vertebra MGPT 13802/10 (caudal)	97
Length of centrum of vertebra MGPT 13802/10 (caudal)	70
Width of centrum of vertebra MGPT 13802/11 (caudal	94
Height of centrum of vertebra MGPT 13802/10 (caudal)	94
Length of centrum of vertebra MGPT 13802/10 (caudal)	64
Width of centrum of vertebra 13802/12 (caudal)	64
Height of centrum of vertebra 13802/12 (caudal)	65
Length of centrum of vertebra 13802/12 (caudal)	36

Lumbar vertebra: Robust vertebra displaying a ventral crest-like keel; dorsolateral and ventrolateral borders concave dorsoventrally and anteroposteriorly; transverse processes broken at base.

Caudal vertebrae: I was able to identify four caudal vertebrae, all of which have eroded borders; the caudal vertebra 13802/9 has strong attachment sites for chevrons and complete neural arch with neural process broken (Fig. 8C, D).

Ribs: Thirteen ribs have been described and measured by Portis (1885) and six of them are figured in Figure 8E. The ribs are slender; only one rib is two-headed with a small, pointed tuberculum and wide, flat capitulum. Attachments for muscles are not marked, suggesting that thoracic musculature was not strong.

Humerus: I did not find any distinguishing features in the humerus of *Eschrichtioides gastaldii*. The head of the humerus (Fig. 9A) is round and protrudes dorsally; the deltopectoral crest is not pronounced and has a triangular shape in lateral view. The distal end of the humerus includes a facet for the articulation with the ulna and a facet for the articulation with the radius. The ulnar facet is orientated posteriorly; the radial facet is transverse with respect to the long axis of the humerus.

Ulna: The ulna is slightly longer than the humerus (Fig. 9B); it is a slender bone with triangular olecranon process. The diaphysis is slightly curved and the distal epiphysis is broad and has a round border.

Manus: Only a few phalanges are figured by Portis (1885). I was unable to find those bones in the MRSN.
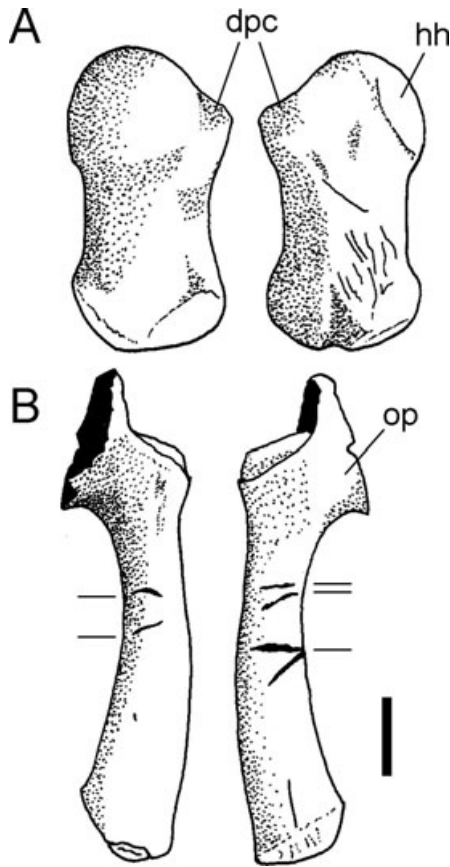
Figure 9. *Eschrichtioides gastaldii* **gen. nov., comb. nov.**: forelimb (redrawn from Portis, 1885). A, lateral and medial views of humerus. B, lateral and medial views of ulna (lateral view). Scale bar = 100 mm. Horizontal lines indicate shark bite marks discussed by Bianucci *et al.* (2002).

COMPARATIVE ANALYSIS

The overall morphology of the skull of *Eschrichtioides gastaldii* is very close to that of the Cetotheriidae with the following exceptions: (1) the anterior border of the supraoccipital is much wider and rounder (in Cetotheriidae, the anterior border of the supraoccipital is triangular with rounded apex in dorsal view); (2) the supraorbital process of the frontal is abruptly depressed from the interorbital region of the frontal (in Cetotheriidae it gently descends from the interorbital region); (3) the ascending temporal crest located over the supraorbital process of the frontal projects sharply posteriorly in the vicinity of the orbit (in Cetotheriidae it forms an oblique line for muscular attachment from the postorbital corner of the orbit to the anteromedial portion of the supraobrital process; this character can only be assessed for *Cetotherium rathkei* because the supraorbital process is lacking in *Metopocetus durinasus* and reconstructed in *Mixocetus elysius*); (4) the

dentary of *E. gastaldii* differs from that of *C. rathkei* in having a satellite process, and higher condyle and angular processes (in *C. rathkei* the angular process projects slightly posteriorly, a feature developed to a greater extent in *Herpetocetus* Van Beneden, 1872).

Cetotheres described by Kellogg (1965, 1968: *Parietobalaena palmeri*, *Diorocetus hiatus*, *Pelocetus calvertensis* and *Aglaocetus patulus*) consistently differ from *E. gastaldii* in having an acutely triangular anterior border of supraoccipital, supraorbital process of frontal gently descending from the interorbital region of the frontal, short and broad (if present) ascending process of the maxilla, dentary lacking satellite process and mylohyoidal concavity on the medial side of the dentary, mandibular condyle facing posteriorly, and slender zygomatic process of the squamosal. Moreover, in such cetotheres as *Pelocetus calvertensis*, *Parietobalaena palmeri*, *Diorocetus hiatus* (Kellogg, 1965, 1968) and *Isanacetus laticephalus* Kimura & Ozawa, 2002, the parietal exposition at vertex is very long whereas in *E. gastaldii* it is shorter but wider.

Eschrichtioides gastaldii differs from the genus *Eomysticetus* Sanders & Barnes, 2002 in having a broader and rounder anterior border of the supraoccipital, presence of the satellite process in the dentary, mylohyoidal concavity in the dentary, shorter and stockier zygomatic process of the squamosal, supraorbital process of the frontal abruptly depressed from the interorbital region of the frontal, and long ascending process of the maxilla.

Eschrichtioides gastaldii differs from the genus *Micromysticetus* Sanders & Barnes, 2002 in being of larger size, in the lack of secondary squamosal fossa, and in having a shorter and stockier zygomatic process of the squamosal and a longer posterior process of the periotic.

With respect to Balaenopteridae, *E. gastaldii* shows many differential morphological features including: strong bulging of parietal and squamosal in the temporal fossa, short zygomatic process of the squamosal, rounder and wider anterior border of supraoccipital, bilateral tubercle on the dorsal surface of the supraoccipital, longitudinally shorter supraorbital process of the frontal, deeper skull, satellite process on dentary, and higher condyle and angular process.

Eschrichtioides gastaldii differs from Balaenidae and Neobalaenidae in having straight rostrum, bilateral tubercle on the dorsal surface of the supraoccipital, bulging of parietal and squamosal in the temporal fossa, presence of ascending process of the maxilla, supraorbital process of the frontal abruptly depressed from the interorbital region of the frontal, satellite process and high angular process of the dentary, absence of torsion at the anterior end of the dentary, and cervical vertebrae free.

Eschrichtioides gastaldii shares with Cetotheriidae the bulging of the parietal and squamosal in the temporal fossa, the short zygomatic process of the squamosal, the interorbital region of the frontal reduced to a subtle sheet of bone surrounding the ascending process of the maxilla, and the presence of a bilateral prominence on the dorsal surface of the supraoccipital.

Eschrichtioides gastaldii shares with Balaenopteridae the abruptly depressed supraorbital process of the frontal. It shares with Balaenidae the presence of a ventral lamina of the pterygoid, deep skull and short zygomatic process of the squamosal.

Eschrichtioides gastaldii differs from *Eschrichtius robustus* in having a straight rostrum, smaller nasals, smaller overall size, coronoid process and post-coronoid fossa more developed, dentary much more bowed, and bilateral tubercle on the supraoccipital less developed. It differs from the *Eschrichtius* sp. described by Ichishima *et al*. (2006) in being much smaller and in having more rounded anterior border of the supraoccipital; however, the Japanese specimen is very incomplete and further comparisons are not possible.

PHYLOGENETIC ANALYSIS

In the present paper, a new cladistic analysis of mysticetes is developed for the following reasons: to aid our understanding of (1) the phylogenetic relationships of *Eschrichtioides gastaldii*, (2) the phylogenetic position of Eschrichtiidae and (3) the phylogenetic positions of Balaenopteridae and Cetotheriidae with respect to Eschrichtiidae.

METHODS

The phylogenetic analysis was carried out using 165 morphological characters scored for 35 taxa and represents the most inclusive phylogenetic study of the mysticetes yet attempted. A list of the examined specimens together with their geological age, repository and relevant literature is provided in Appendix 1 together with a character list and the taxon × character matrix. The taxonomic sample was chosen in such a way as to include representatives of all the mysticete radiations (aetiocetids, eomysticetoids, balaenids, neobalaenids, eschrichtiids, balaenopterids and several cetotheres). Three of the taxa used in the phylogenetic analysis need some comment. The Mount Pulgnasco whale was described by Cortesi (1819) and by subsequent authors (Cuvier, 1823; Van Beneden, 1875; Strobel, 1881) up to its destruction during a bombing run over the Museo di Storia Naturale, Milano, where it was stored, during the Second World War; it consisted of a nearly com-

plete skeleton of a basal balaenopterid which was used also by Zeigler, Chan & Barnes (1997) in their analysis of the phylogenetic relationships of *Parabalaenoptera baulinensis*. The specimens indicated as MCA 240536 and MPST 240505 represent, respectively, a Pliocene basal balaenopterid and a late Miocene balaenopterid whose descriptions have been provided elsewhere (Bisconti, 2003a).

The characters used in the present work are derived partly from my own observations on the specimens and partly from the literature. In particular, I relied on information provided in the following papers: Miller (1923), Kellogg (1928, 1931, 1965, 1968), Fraser & Purves (1960), Barnes & McLeod (1984), McLeod, Whitmore & Barnes (1993), Fordyce (1994), Geisler & Luo (1996, 1998), Messenger & McGuire (1998), Luo & Gingerich (1999), Bisconti (2001, 2003a), Kimura & Ozawa (2002), Sanders & Barnes (2002) and Geisler & Sanders (2003),

In constructing the character list, close attention was paid to incorporating as much data about individual variation as possible. In particular, it was possible to assess the variation of the skull architecture (relationships of the bone in the temporal fossa, variation of tympanic bulla and of periotics) in living eschrichtiids, balaenopterids and balaenids and in some fossil taxa (*Parietobalaena palmeri*, *Diorocetus hiatus*, *Metopocetus durinasus*). This assessment allowed the exclusion of certain characters from the list because these characters were highly variable. In particular, I excluded features from the tympanic bulla (shape of the anteromedial corner, shape of the anterolateral border of the tympanic wall) and from the parietal (relationships of parietal to frontal and to squamosal due to high variability in the grey whales, especially once the North Atlantic record is taken into account). The procedure for the assessment of the amount of individual variation is described in Bisconti (2003a).

The cladistic analysis was carried out with PAUP 4.0b10 (Swofford, 2002) using *Protocetus atavus* Fraas, 1904 and *Georgiacetus vogtlensis* Hulbert *et al*., 1998 as outgroup taxa. Character states were treated as unordered and unweighted under the ACCTRAN character state optimization. The search for the most parsimonious cladograms was made by tree–bisection–reconnection (TBR) with ten replicates and one tree held at each step during stepwise addition followed by bootstrap analysis with 1000 replicates. A randomization test was performed by PAUP to assess the distance of the results from 10 000 cladograms sampled equiprobably from the set of all possible trees generated from the original matrix. The randomization test was performed by PAUP by combining ten different randomization analyses generating 1000 equiprobable cladograms each. The agreement between phyloge-
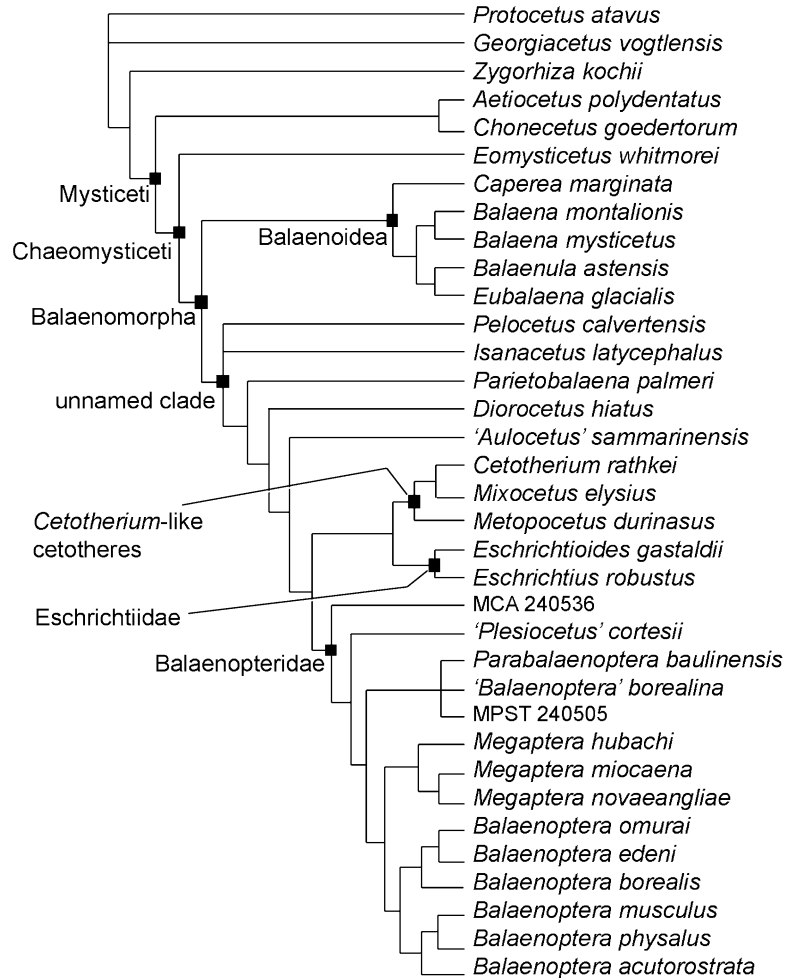
Figure 10. Phylogenetic relationships of ***Eschrichtioides gastaldii*** **gen. nov., comb. nov.**. Strict consensus tree from nine equally most-parsimonious trees. Tree statistics: tree length, 503 steps; Consistency Index (CI), 0.5447; Retention Index (RI), 0.8115; Homoplasy Index (HI), 0.4553; Rescaled CI, 0.4421.

netic results and stratigraphic occurrence of the taxa was evaluated by calculating the Stratigraphic Consistency Index (SCI) developed by Huelsenbeck (1994). This index is a number ranging from 0 to 1, the latter being the maximum possible agreement between the position of taxa in the cladogram and their stratigraphic age; it is obtained by dividing the number of stratigraphically consistent nodes against the total number of nodes of the cladogram excluding the root; the latter is calculated as the total number of taxa minus 2 (for discussions on the SCI see Siddall, 1995; Clyde & Fisher, 1997; Hitching & Benton, 1997).

RESULTS

General patterns

The TBR search found one island of trees containing nine cladograms which were 503 steps long. A strict consensus of the most parsimonious trees is presented in Figure 10 and tree statistics are provided in the corresponding caption. The following phylogenetic patterns are evident in the strict consensus tree:

1. The suborder Mysticeti is monophyletic, with Aetiocetidae and Eomysticetidae its most primitive families.
2. Eomysticetidae is the sister group of a clade (Balaenomorpha *sensu* Geisler & Sanders, 2003) formed by two large branches. One includes Balaenidae and Neobalaenidae and corresponds to the superfamily Balaenoidea Gray, 1825; the other includes Balaenopteridae, Eschrichtiidae and cetotheres.
3. Balaenoidea includes Neobalaenidae and Balaenidae. The taxa included in the present study are too few to completely characterize the phylogenetic relationships among balaenids, which are treated elsewhere (Bisconti, 2005); however, from

the present work it appears that the genus *Balaenula* Van Beneden, 1872 is more closely related to the right whale (genus *Eubalaena*) than to the bowhead whale (genus *Balaena* Linnaeus, 1758), and that *Caperea marginata* (Neobalaenidae) is sister taxon of Balaenidae.

4. Cetotheres are paraphyletic. *Pelocetus*, *Isanacetus*, *Parietobalaena*, *Diorocetus* and *Titanocetus sammarinensis* are placed at the base of the balaenopteroid clade, while Cetotheriidae (*Cetotherium*, *Mixocetus* and *Metopocetus*) and eschrichtiids form the monophyletic sister group of Balaenopteridae.

5. Eschrichtiidae and Cetotheriidae are monophyletic to the exclusion of balaenopterids and Early and Middle Miocene cetotheres. In particular, from the present analysis, *Cetotherium rathkei* and *Mixocetus elysius* are sister taxa to the exclusion of *Metopocetus durinasus*.

6. *Eschrichtioides gastaldii* and *Eschrichtius robustus* form a monophyletic group (family Eschrichtiidae) that represents the sister taxon of Cetotheriidae. Thus, Eschrichtiidae is excluded

from belonging to Balaenopteridae and is more closely related to Cetotheriidae.

7. The phylogenetic relationships of Balaenopteridae will be treated elsewhere (Bisconti, in press) and will not be explored here. It is sufficient to note that this study reinforces the systematics of Balaenopteridae provided by Zeigler *et al*. (1997) in which three subfamilies were considered valid: Balaenopterinae (including the genus *Balaenoptera*), Megapterinae (including the genus *Megaptera*) and Parabalaenopterinae (originally including only the genus *Parabalaenoptera* Zeigler *et al*., 1997 but now including also MPST 240505). Not included within these subfamilies are two stem balaenopterids: '*Plesiocetus*' *cortesii* and MCA 240536.

Bootstrap analysis

The 50%-majority rule cladogram supports the above results only partially (Fig. 11). In the bootstrap tree the genera *Balaenoptera*, *Megaptera* and *Parabalaenoptera* collapse forming an unresolved node; the basal position of MCA 240536 and of '*Plesiocetus*'
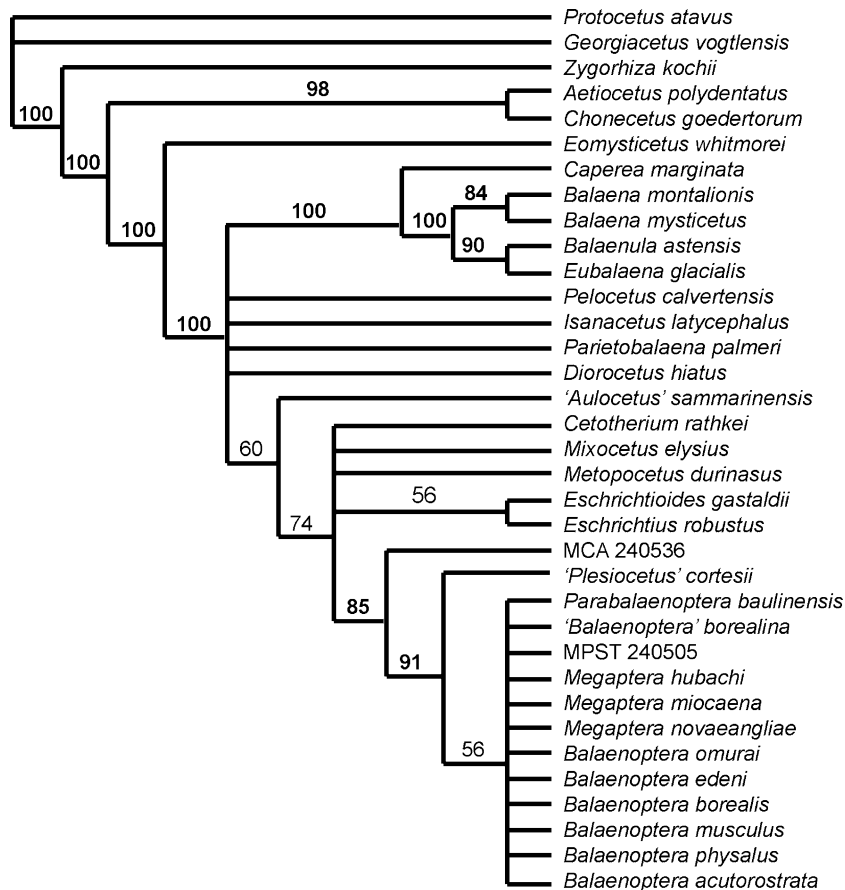

Figure 11. Fifty-% majority-rule strict consensus bootstrap tree; tree statistics: CI, 0.568; RI, 0.7582; HI, 0.5173; Rescaled CI, 0.3659. Numbers above branch are bootstrap support values; numbers in bold are values higher than 80%.

cortesii is confirmed as is the sister group relationship of *Titanocetus sammarinensis* and the clade including Eschrichtiidae, Balaenopteridae and *Cetotherium*-like cetotheres. The monophyly of Balaenopteridae, Eschrichtiidae, Balaenoidea, Balaenomorpha, Chaeomysticeti, Aetiocetidae and Mysticeti is supported by the present analysis. High bootstrap values support the monophyly of Mysticeti, Chaeomysticeti, Balaenomorpha, Balaenoidea, Aetiocetidae and Balaenopteridae. In conclusion, the overall pattern of mysticete phylogeny as depicted by the most parsimonious strict consensus tree of Figure 10 is confirmed by the bootstrap analysis but more evidence needs to be provided to support also the species relationships among Balaenopteridae, Cetotheriidae, and such archaic taxa as *Pelocetus calvertensis*, *Diorocetus hiatus*, *Parietobalaena palmeri* and *Isanacetus laticephalus*.

Randomization test and SCI
The randomization test provided highly significant results. The mean length of 10 000 trees generated equiprobably from the matrix used in the cladistic search was 1297.3887 steps with a standard deviation of 46.763, which is much higher than that of the most parsimonious trees found by TBR (503 steps). Thus, the probability that the TBR results were due to chance was significantly low ($P < 0.0001$).

Calculation of the SCI was negatively influenced by the presence of two unresolved polytomies in the strict consensus tree. These polytomies lowered to 25 the number of nodes for which it was possible to assess the stratigraphic consistency from a total of 33. The SCI of the strict consensus TBR tree of Figure 10 was 0.757. The SCI calculated for the cladograms found by Kimura & Ozawa (2002) ranged from 0.3 to 0.5 depending on the number of taxa and on the balaenid species included. The SCI calculated for the cladogram found by Dooley, Fraser & Luo (2004) was 0.562. In conclusion, despite the negative influence of the unresolved polytomies, the SCI of the most parsimonious trees found in the present work is comparatively much higher than those of other recent studies, suggesting that the present phylogenetic results are in better agreement with the stratigraphic occurrence of the taxa.

DISCUSSION

Eschrichtioides gastaldii is the most complete eschrichtiid fossil to be fully described. Another new fossil eschrichtiid genus from the Late Miocene of southern Italy has been recently described by Bisconti & Varola (2006) that is represented by a single dentary; a third taxon has been briefly outlined by Deméré *et al*. (2005). Until a few years ago, there was no fossil record older than late Pleistocene for Eschrichtiidae (Barnes & McLeod, 1984; Ichishima *et al*., 2006) but now it is clear that some aspects of the evolutionary history of this family can be outlined using fossils.

As discussed in a previous section, the phylogenetic relationships of Eschrichtiidae have been resolved in different ways by morphologists and molecular biologists with the consequent absence of a shared view. The phylogenetic results presented in the present work do not support the molecular-based conclusion that the living *Eschrichtius robusus* is part of Balaenopteridae. Rather, my results support the monophyly of Eschrichtiidae and Cetotheriidae to the exclusion of all the other mysticete taxa. This result agrees with the early interpretation of Miller (1923) and Kellogg (1928) who thought that the living grey whale was a living fossil closely related to the cetotheres. In this sense, *Eschrichtius robustus* should be considered as the last relict survivor of a wider radiation of Cetotheriidae and eschrichtiids that started at least in the Middle Miocene. Accepting this hypothesis would result in assigning the highest priority to the conservation of the living populations of *Eschrichtius robustus* (Bisconti, 2005).

Eschrichtioides gastaldii represents an evident link between Eschrichtiidae and Cetotheriidae. Its skull morphology grossly resembles that of *Cetotherium rathkei* in its main features. The principal differences between *E. gastaldii* and Cetotheriidae lies in mandibular morphology. In particular, the presence of a satellite process, the mylohyoidal concavity on the medial side, the high condyle and the high angular process all make *E. gastaldii* more closely related to Eschrichtiidae than to *Cetotherium*-like forms. In this sense, *E. gastaldii* is not close to the basal stock of Eschrichtiidae, representing a derived species whose feeding adaptations (as expressed by the mandibular morphology) are well suited for performing the suction feeding observed in the living grey whale (Sanderson & Wassersug, 1993 and literature therein). The presence of a well-developed postcoronoid crest and fossa suggests that *E. gastaldii* used adductor muscles such as the temporalis in a more active way than *Eschrichtius robustus*.

The presence of *Eschrichtioides gastaldii* in the Early Pliocene of the Mediterranean Basin shows that the Mediterranean trophic web was more complex than that at present. In fact, current mysticete populations of the Mediterranean include only one resident species, the fin whale (*Balaenoptera physalus*), and several occasional species unable to form stable populations. In the Pliocene, balaenids, balaenopterids and eschrichtiids were inhabiting the Mediterranean Basin (Bisconti, 2003a); this means that trophic resources were abundant and were

exploited by mysticetes through at least three different feeding behaviours: continuous and intermittent ram feeding (respectively adopted by balaenids and balaenopterids), and intermittent suction feeding (eschrichtiids). The reasons for the oversimplification of the modern Mediterranean trophic web is unclear. However, theoretical models explaining the reduction of mysticete diversity over the last 5 Myr have begun to appear (Bisconti, 2003b). Further field and theoretical study is critically necessary to test the hypotheses emerging from these studies.

CONCLUSIONS

1. *Eschrichtioides gastaldii* is a new eschrichtiid taxon closely related to the living grey whale, *Eschrichtius robustus*.
2. Eschrichtiidae is monophyletic with three genera belonging to Cetotheriidae (*Cetotherium rathkei*, *Mixocetus elysius*, *Metopocetus durinasus*) to the exclusion of the other mysticete taxa.
3. Eschrichtiidae and Cetotheriidae are the sister group of Balaenopteridae.
4. The feeding adaptations of *E. gastaldii* (as derived from its mandibular morphology) are the same as those of *Eschrichtius robustus*, suggesting that it fed through an intermittent suction mechanism similar to that of the living grey whale, although a fuller biomechanical characterization of the feeding mechanism of living and fossil eschrichtiids is yet to come.
5. The phylogenetic position of *Eschrichtius robustus* suggests that this taxon is the last relict survivor of a major radiation that occurred in the Pliocene. From this conclusion it is recommended that highest priority conservation strategies be adopted for the remaining populations of this relict species.

ACKNOWLEDGEMENTS

REFERENCES

Baker AN. 1985. Pygmy right whale – *Caperea marginata*. In: Ridgway SM, Harrison R, eds. *Handbook of marine mammals*, Vol. 3. London: Academic Press, 345–355.

Barnes LG, Kimura M, Furusawa H, Sawamura H. 1995. Classification and distribution of Oligocene Aetiocetidae (Mammalia; Cetacea; Mysticeti) from western North America and Japan. *Island Arc* **3:** 392–431.

Barnes LG, McLeod SA. 1984. The fossil record and phyletic relationships of Gray Whales. In: Jones ML, Leatherwood S, Swartz S, eds. *The gray whale*. Orlando: Academic Press, 3–32.

Beddard FE. 1901. Contribution towards a knowledge of the osteology of the pigmy whale (*Neobalaena marginata*). *Transactions of the Zoological Society* **16:** 87–108.

Bianucci G, Bisconti M, Landini W, Storai T, Zuffa M, Giuliani S, Mojetta A. 2002. Mediterranean white shark–cetaceans interactions through time: a comparison between Pliocene and Recent data. In: Vacchi M, La Mesa G, Serena F, Séret B, eds. *Proceedings of the 4th European Elasmobranch Association Meeting* Livorno: ICRAM, ARPAT & SFI, 33–48.

Bisconti M. 2000. New description, character analysis and preliminary phyletic assessment of two Balaenidae skulls from the Italian Pliocene. *Palaeontographia Italica* **87:** 37–66.

Bisconti M. 2001. Morphology and postnatal growth trajectory of rorqual petrosal. *Italian Journal of Zoology* **68:** 87–93.

Bisconti M. 2002. An early Late Pliocene right whale (genus *Eubalaena*) from Tuscany (Central Italy). *Bollettino della Società Paleontologica Italiana* **41:** 83–91.

Bisconti M. 2003a. Systematics, paleoecology, and paleobiogeography of archaic mysticetes from the Italian Neogene. Doctoral Dissertation, University of Pisa.

Bisconti M. 2003b. Evolutionary history of Balaenidae. *Cranium* **20:** 9–50.

Bisconti M. 2005. Evolutionary history of the gray whale. In: *Primo Congresso dei Biologi Evoluzionisti Italiani*. Ferrara: Università degli Studi di Ferrara, 16.

Bisconti M. 2006. *Titanocetus*, a new baleen whale from the Middle Miocene of northern Italy (Mammalia, Cetacea, Mysticeti). *Journal of Vertebrate Paleontology* **26:** 344–364.

Bisconti M, Varola A. 2000. Functional hypothesis on an unusual mysticete dentary with double coronold process from the Miocene of Apulia and its systematic and behavioural implications. *Palaeoncographia Italica* **87:** 19–35.

Bisconti M, Varola A. 2006. The oldest eschrichtiid mysitete and a new morphological diagnosis of Eschrichtiidae (Gray Whales). *Rivista Italiana di Paleontologia e Stratigrafia* **112:** 447–457.

Bouetel V, de Muizon C. 2006. The anatomy and relationships of *Piscobalaena nana* (Cetacea, Mysticeti), a Cetotheriidae s.s. from the early Pliocene of Peru. *Geodiversitas* **28:** 319–395.

Brandt JF. 1873. Untersuchungen uber die fossilen und subfossilen Cetaceen Europas. *Memoires de l'Academie imperiale des Sciences, St. Pétersburg* **7:** 1–54.

Burns JJ, Montague JJ, Cowles CJ, eds. 1993. The Bowhead whale. *The Society for Marine Mammalogy, Special Publication* **2:** 1–787.

Capellini G. 1900. Balenottera miocenica della Repubblica di San Marino. *Atti della Reale Accademia dei Lincei* **5:** 233–235.

Caretto PG. 1970. La balenottera delle sabbie plioceniche di Valmontasca (Vigliano d'Asti). *Bollettino della Società Paleontologica Italiano* **9:** 3–750.

Clapham PJ, Mead JG. 1999. *Megaptera novaeangliae.* *Mammalian Species* **604:** 1–9.

Clyde WC, Fisher DC. 1997. Comparing the fit of stratigraphic and morphologic data in phylogenetic analysis. *Paleobiology* **23:** 1–19.

Cortesi G. 1819. *Saggi geologici degli stati di Parma e Piacenza dedicati a sua Maestà la principessa imperiale Maria Luigia arciduchessa d'Austria duchessa di Parma Piacenza Guastalla ecc. ecc. ecc*. Piacenza: Torchj del Majno.

Cummings WC. 1985. Right whales – *Eubalaena glacialis* and *Eubalaena australis*. In: Ridgway SM, Harrison R, eds. *Handbook of marine mammals*, Vol. 3. London: Academic Press, 275–304.

Cuvier G. 1823. Recherches sur les ossemens fossiles, où l'on rètablit les caractères de plusieurs animaux dont les révolutions du globe ont détruit les espéces. **5:** 309–398.

Dathe F. 1983. *Megaptera hubachi* n. sp., ein fossiler Bartenwal aus marinen Sandsteinschichten des tieferen Pliozäns Chiles. *Zeitscrift für Geological Wiss* **11:** 813–852.

Demére TA, Berta A. 2003. A new species of baleen whale (Cetacea: Mysticeti) from the Pliocene of California and its implications for higher mysticete phylogenetic relationships. *Journal of Vertebrate Paleontology* **23:** 45A.

Demére TA, Berta A, McGowen MR. 2005. The taxonomic and evolutionary history of fossil and modern balaenopteroid mysticetes. *Journal of Mammalian Evolution* **12:** 99–143.

Dooley AC Jr, Fraser NC, Luo Z. 2004. The earliest known member of the rorqual-gray whale clade (Mammalia, Cetacea). *Journal of Vertebrate Paleontology* **24:** 453–463.

Ferrero E, Pavia G. 1996. La successione marina previllanoviana. In: Carraro F, ed. Revisione del Villafranchiano nell'area-tipo di Villafranca d'Asti. *Il Quaternario* **9:** 36–38.

Fordyce RE. 1994. *Waipatia maerewhenua*, new genus and new species, Waipatiidae, new family, an archaic late Oligocene dolphin (Cetacea: Odontoceti: Platanistoidea) from New Zealand. *Proceedings of the san Diego Society of Natural History* **29:** 147–176.

Fordyce RE, Barnes LG. 1994. The evolutionary history of whales and dolphins. *Annual Review of Earth and Planetary Science* **22:** 419–455.

Fraser FC, Purves PE. 1960. Hearing in cetaceans. *Bulletin of the British Museum (Natural History), Zoology* **7:** 1–140.

Gambell R. 1985a. Sei whale – *Balaenoptera borealis*. In: Ridgway SM, Harrison R, eds. *Handbook of marine mammals*, Vol. 3. London: Academic Press, 155–170.

Gambell R. 1985b. Fin whale – *Balaenoptera physalus*. In: Ridgway SM, Harrison R, eds. – *Handbook of marine mammals*, Vol. 3. London: Academic Press, 171–192.

Geisler JH, Luo Z. 1996. The petrosal and inner ear of *Herpetocetus* sp. (Mammalia: Cetacea) and their implications for the phylogeny and hearing of archaic mysticetes. *Journal of Paleontology* **70:** 1045–1066.

Geisler JH, Luo Z. 1998. Relationships of Cetacea to terrestrial Ungulates and the evolution of cranial vasculature in Cete. In: Thewissen JGM, ed. *The emergence of whales: evolutionary patterns in the origin of Cetacea*. New York: Plenum Press, 163–212.

Geisler JH, Sanders AE. 2003. Morphological evidence for the phylogeny of Cetacea. *Journal of Mammalian Evolution* **10:** 23–129.

Hitching R, Benton MJ. 1997. Congruence between parsimony and stratigraphy: comparisons of three indices. *Paleobiology* **23:** 20–32.

Huelsenbeck JP. 1994. Comparing the stratigraphic record to estimates of phylogeny. *Paleobiology* **20:** 470–483.

Hulbert RC Jr. 1998. Postcranial osteology of the North American Middle Eocene protocetid *Georgiacetus*. In: Thewissen JGM, ed. *The emergence of whales*. New York: Plenum Press, 235–267.

Hulbert RC Jr, Petkewich RM, Bishop GA, Bukry D, Aleshire DP. 1996. A new Middle Eocene protocetid whale (Mammalia: Cetacea: Archaeoceti) and associated biota from Georgia. *Journal of Paleontology* **72:** 907–927.

Ichishima H, Sato E, Sagayama T, Kimura M. 2006. The oldest record of Eschrichtiidae (Cetacea: Mysticeti) from the Late Pliocene, Hokkaido, Japan. *Journal of Paleontology* **80:** 367–379.

Junge GCA. 1950. On a specimen of the rare fin whale, *Balaenoptera edeni* Anderson, stranded on Pulu Sugi near Singapore. *Zoologische Verhand* **9:** 3–26.

Kellogg R. 1922. Description of the skull of *Megaptera miocaena*, a fossil humpback whale from the Miocene diatomaceous earth of Lompoc; California. *Proceedings of The United States National Museum* **61:** 1–18.

Kellogg R. 1928. The history of whales – their adaptation to life in the water. *Quarterly Review of Biology* **3:** 29–76, and 174–208.

Kellogg R. 1931. Pelagic mammals from the Temblor Formation of the Kern River Region, California. *Proceedings of the California Academy of Sciences* **19:** 217–397.

Kellogg R. 1936. A review of the Archaeoceti. *Carnegie Instution Washington* **482:** 1–366.

Kellogg R. 1965. A new whalebone whale from the Miocene Calvert Formation. *United States National Museum Bulletin* **247:** 1–45.

Kellogg R. 1968. Fossil marine mammals from the Miocene Calvert Formation of Maryland and Virginia. *United States National Museum Bulletin* **247:** 103–197.

Kimura T, Ozawa T. 2002. A new cetothere (Cetacea: Mysticeti) from the Early Miocene of Japan. *Journal of Vertebrate Paleontology* **22:** 684–702.

Luo Z, Gingerich PD. 1999. Terrestrial Mesonychia to aquatic Cetacea: transformation of the basicranium and evolution of hearing in whales. *University of Michigan Papers in Paleontology* **31:** 1–98.

McLeod SA, Whitmore FC Jr, Barnes LG. 1993. Evolutionary relationships and classification. In: Burns JJ,

Montague JJ, Cowles CJ, eds. The bowhead whale. *The Society for Marine Mammalogy, Special Publication* **2:** 45–70.

Messenger S, McGuire JA. 1998. Morphology, molecules, and the phylogenetics of Cetaceans. *Systematic Biology* **47:** 90–124.

Miller GS. 1923. The telescoping of the cetacean skull. *Smithsonian Miscellaneous Collections* **76:** 1–70.

Monegatti P, Raffi S. 2001. Taxonomicc diversity and stratigraphic distribution of Mediterranean Pliocene bivalves. *Palaeogeography, Palaeoecology, Palaeoclimatology* **165:** 171–193.

Pilleri G. 1986. *Beobachtungen an den fossilen Cetaceen des Kaukasus.* Ostermundigen: Brain Anatomy Institute.

Portis A. 1885. Catalogo descrittivo dei Talassoterii rinvenuti nei terreni terziari del Piemonte e della Liguria. *Memorie della Reale Accademia delle Scienze di Torino* **37:** 247–365.

Raffi S, Stanley SM, Marasti R. 1985. Biogeographic patterns and Plio-Pleistocene extinctions of Bivalvia in the Mediterranean and Southern North Sea. *Paleobiology* **11:** 368–388.

Reeves RR, Leatherwood S. 1985. Bowhead whale – *Balaena mysticetus.* In: Ridgway SM, Harrison R, eds. *Handbook of marine mammals*, Vol. 3. London: Academic Press, 305–344.

Sacco F. 1890. Sopra una mandibola di Balaenoptera dell'Astigiana. *Atti della Regia Accademia delle Scienze di Torino* **25:** 3–8.

Sanders AE, Barnes LG. 2002. Paleontology of the late oligocene ashley and chandler bridge formations of South Carolina, 3: eomysticetidae, a new family of primitive mysticetes (Mammalia: Cetacea). In: Emry RJ, ed. Cenozoic mammals of land and sea: tributes to the career of Clayton E. Ray. *Smithsonian Contribution to Paleobiology* **93:** 313–356.

Sanderson LR, Wassersug R. 1993. Convergent and alternative designs for vertebrate suspension feeding. In: Hanken J, Hall BK, eds. *The skull. Volume 3: Functional and evolutionary mechanisms*. Chicago: University Press of Chicago, 37–112.

Siddall ME. 1995. Stratigraphic consistency and the shape of things. *Systematic Biology* **45:** 111–115.

Stewart BS, Leatherwood S. 1985. Minke whale – *Balaenoptera acutorostrata.* In: Ridgway SM, Harrison R, eds. *Handbook of marine mammals*, Vol. 3. London: Academic Press, 91–136.

Strobel P. 1881. *Iconografia comparata delle ossa fossili del gabinetto di storia naturale dell'Università di Parma.* Parma: Libreria Editrice Luigi Battei.

Swofford DL. 2002. *PAUP – Phylogenetic Systematics Using Parsimony.* Beta Documentation. Washington, DC: Laboratory of Molecular Systematics, Smithsonian Institution. Available at http://paup.csit.fsu.edu/

True FW. 1904. The whalebone whales of the western North Atlantic. *Smithsonian Contributions to Knowledge* **33:** 1–322.

Uhen MD. 1998. Middle to Late Eocene basilosaurines and dorudontines. In: Thewissen JGM, ed. The emergence of whales. *Evolutionary patterns in the origin of Cetacea*. New York: Plenum Press, 29–63.

Van Beneden P-J. 1875. Le squelette de la baleine fossile du Musée de Milan. *Bulletin de l'Academie Royale des Sciences du Belgique* **40:** 736–758.

Van Beneden P-J. 1882. Description des ossements fossiles des environs d'Anvers. Genre *Plesiocetus. Annales du Museum Royale d'Histoire Naturelle du Belgique* **9:** Atlas.

Wada S, Oishi M, Yamada TK. 2003. A newly discovered species of living baleen whale. *Nature* **426:** 278–281.

Winn HE, Reichley NE. 1985. Humpback whale – *Megaptera novaeangliae.* In: Ridgway SM, Harrison R, eds. *Handbook of marine mammals*, Vol. 3. London: Academic Press, 241–274.

Wolman AA. 1985. Gray whale – *Eschrichtius robustus.* In: Ridgway SM, Harrison R, eds. *Handbook of marine mammals*, Vol. 3. London: Academic Press, 67–90.

Yochem PK, Leatherwood S. 1985. Bowhead whale – *Balaena mysticetus.* In: Ridgway SM, Harrison R, eds. *Handbook of marine mammals*, Vol. 3. London: Academic Press, 305–354.

Zeigler CV, Chan GL, Barnes LG. 1997. A new Late Miocene balaenopterid whale (Cetacea: Mysticeti), *Parabalaenoptera baulinensis*, (new genus and species) from the Santa Cruz Mudstone, Point Reyes Peninsula, California. *Proceedings of the California Academy of Sciences* **50:** 115–138.

APPENDIX 1

LIST OF SPECIMENS EMPLOYED IN THE CLADISTIC ANALYSIS

Protocetus atavus: SMNS 11084 (holotype); Middle Eocene). *Georgiacetus vogtlensis*: Hulbert *et al*. (1996; Hulbert 1998); Middle Eocene. *Zygorhiza kochii*: USNM 4748, 16638, 449538; Kellogg (1936), Uhen (1998); Late Eocene. *Chonecetus goedertorum*: Barnes *et al*. (1995); Late Oigocene. *Aetiocetus polydentatus*: Barnes *et al*. (1995); Late Oligocene. *Eomysticetus whitmorei*: ChM PV4253 (holotype), Sanders & Barnes (2002); Late Oligocene. *Caperea marginata*: AMNH AMO 36692; IRSN 1536; Baker (1985), Beddard (1901); Recent. *Balaena mysticetus*: USNM 257513; ZML 1680, 3997, 2563, 2001, 'Balaena japonica' (1-2); Bisconti (2003b), Burns, Montague & Cowles (1993), Reeves & Leatherwood (1985); Recent. *Balaena montalionis*: MSNT MC CF 31 (holotype); Bisconti (2000, 2003b); Early Pliocene. *Balaenula astensis*: MSNT MC CF 35 (holotype); Bisconti (2000); Early Pliocene. *Eubalaena glacialis*: AMNH 42752, 256803, 90241; MSNT 264; USNM 267612, 3339990, 23077, 301637; Bisconti (2003b), Cummings (1985), True (1904); Recent. *Pelocetus calvertensis*: USNM 11976 (holotype); Kellogg (1965); Middle Miocene. *Isanacetus laticephalus*: Kimura & Ozawa (2002);

Early Miocene. *Parietobalaena palmeri*: AMNH 128885; USNM 10677, 16570, 24883, 10909; Kellogg (1968); Middle Miocene. *Diorocetus hiatus*: USNM 16783 (holotype), 205990; Kellogg (1968); Middle Miocene. *Cetotherium rathkei*: Pilleri (1986); Middle Miocene. *Mixocetus elysius*: Kellogg (1931); Late Miocene. *Metopocetus durinasus*: USNM 60460 (holotype); Kellogg (1968); Late Miocene. *Eschrichtius robustus*: AMNH 181374, 34260, 1750 ('Eschrichtius cephalum'), A; NMB 42001; USNM 364969, 364580, 571931, 364969, 364977, 364970, 364973, 504305; ZML St20350, St13130, 630 ('*Eschrichtius gibbosus*'); Wolman (1985), True (1904); Pleistocene to Recent. *Eschrichtioides gastaldii*: MGPT 13802 (holotype); Portis (1885); Early Pliocene. *Titanocetus sammarinensis*: MGB 9073 1CMC172 (1-6) (holotype); Capellini (1900), Bisconti (2006); Middle Miocene. MCA 240536 (inventory of the Soprintendenza per i Beni Archeologici dell'Emilia Romagna); Bisconti (2003b); Middle Pliocene. The Mount Pulgnasco whale: Cortesi (1819), Cuvier (1823), Van Beneden (1875), Strobel (1881); Middle Pliocene. MPST 240505 (inventory of the Soprintendenza per i Beni Archeologici dell'Emilia Romagna); Bisconti (2003b); Late Miocene. *Balaenoptera borealina*: IRSN CtM775a-b, CtM778, CtM777, CtM774 (type); Van Beneden (1882); Early Pliocene. *Parabalaenoptera baulinensis*: Zeigler *et al*. (1997); Late Miocene. *Megaptera hubachi*: Dathe (1983); Middle Pliocene. *Megaptera miocaena*: Kellogg (1922); Late Miocene. *Megaptera novaeangliae*: AMNH 24679; MSNT 263; USNM 269982, 486175 (1-2), 13656/16252, 21492; ZMA 14964, 14953 (1-2), 14952 (1-2), 14965, 14966, 14967; Clapham & Mead (1999), Winn & Reichley (1985); Recent. *Balaenoptera acutorostrata*: AMNH 181411, 35680; IRSN 1537; MSNT 260, 261; ZMA 12873; Stewart & Leatherwood (1985), True (1904); Recent. *Balaenoptera physalus*: AMNH 35026, 256796; MSNT 251, 252, 253, 258, 255, 257; ZMA 14950 (1-2), 14927 (1-2), 14935 (1-2), 23353, 14947; Gambell (1985b); Recent. *Balaenoptera musculus*: AMNH 234949, 256797, 256798; MSNT 250; ZMA 23356, 23354, 23355, 14946, 14942, 14961; Yochem & Leatherwood (1985), True (1904); Recent. *Balaenoptera edeni*: USNM 504692, 236680 (1-3); Cummings (1985), Junge (1950); Recent. *Balaenoptera omurai*: Wada, Oishi & Yamada (2003); Recent. *Balaenoptera borealis*: USNM 504699, 504698, 504701, 504244, 486174; Gambell (1985a); Recent.

CHARACTER LIST

Character states are from personal observations and literature listed in the Phylogenetic analysis section (see Materials and methods). Some of the characters are commented on or described in detail whenever their concise description may leave room for ambiguous interpretations.

1. Suprameatal area of petrosal: 0, low; 1, high.
2. Pterygoid air sinus: 0, absent; 1, present around the tympanic bulla.
3. Ascending temporal crest: 0, absent; 1, present. The ascending temporal crest represents the anteriormost attachment site for the temporalis muscle and is located on the dorsal surface of the supraorbital process of the frontal or along its posterior border. The position of the temporal crest represents a different character: in fact, the ascending temporal crest is present in all baleen-bearing mysticetes but its position is not the same in all the families. For this reason, the position of the ascending temporal crest is treated separately in character 19.
4. Parietal and squamosal are bulged into the temporal fossa: 0, no; 1, yes.
5. Ascending process of maxilla: 0, absent; 1, present and narrow; 2, present and wide.
6. Plate-like infraorbital process of the maxilla: 0, absent; 1, present.
7. Zygomatic process of maxilla bears a steep face that clearly separates the rostrum from the antorbital process of the frontal: 0, no; 1, yes.
8. Wide and bulbous basioccipital crest: 0, no; 1, yes.
9. Mandibular symphysis: 0, present; 1, absent (groove for mental ligament present).
10. Tympanic membrane: 0, present; 1, modified into glove finger. This is a soft tissue character. Fraser & Purves (1960) found that the tympanic membrane was modified into a glove finger-like shape in all the living mysticetes they analysed.
11. Foramen 'pseudo-ovale': 0, absent; 1, present. The foramen 'pseudo-ovale' has been extensively described by Fraser & Purves (1960), who found it to be an apomorphic development of the foramen ovale of other mammals. It is found in mysticetes only. Its opening is located in different positions among mysticete taxa; the relative position of the foramen 'pseudo-ovale' is treated in character 117.
12. Posterior process of petrosal: 0, absent; 1, present. The posterior process of the petrosal is a character of Neoceti (Luo & Gingerich, 1999). It is developed at different extents among odontocetes and mysticetes. The relative development of the posterior process (in terms of length) is treated in character 23.
13. Sternum: 0, formed by manubrium and several seternebra; 1, formed by manubrium only.
14. Number of ribs attached to the sternum: 0, several pairs; 1, one pair.

15. Teeth in the adult: 0, present; 1, absent.
16. Dental generations developed during embryology: 0, polyophiodonty; 1, monophiodonty.
17. Baleen plates: 0, absent; 1, present.
18. Lateral squamosal crest: 0, absent; 1, present. The lateral squamosal crest is an acute keel developed along the dorsolateral border of the squamosal being continued on the dorsal edge of the zygomatic process of the squamosal; it is evident in many mysticetes with the exclusion of Balaenopteridae where the crest is highly rounded.
19. Temporal crest either partially or entirely on the dorsal surface of the supraorbital process of the frontal: 0, no; 1, yes. This character denotes the position of the temporal crest at a general extent: in balaenopterids, for instance, the ascending temporal crest is located in the anterior border of the supraorbital process of the frontal and is completely included on the dorsal surface of the process; in balaenids it crosses the supraorbital process of the frontal from the postorbital corner to the anteromedial corner; in eomysticetids the position is rather different. This character supports the monophyly of posteomysticetid baleen-bearing mysticetes. In character 90, the relative position is detailed in order to discover subclades among posteomysticetid baleen-bearing mysticetes.
20. Cranio-mandibular joint: 0, dentary and squamosal closely articulate with each other; 1, dentary and squamosal are not closely articulated. A loose articulation is observed in all baleen-bearing mysticetes.
21. Dentary in dorsal view: 0, straight; 1, slightly bowed; 2, strongly bowed.
22. Parietal moved onto the posterior portion of the interorbital region of the frontal: 0, no; 1, yes. Miller (1923) and Kellogg (1928) described the pattern of bone interdigitation observed in cetacean skulls. In mysticetes, they found that in cetotheres and archaic forms the parietal is exposed at the cranial vertex; in such taxa as *Parietobalaena palmeri*, *Diorocetus hiatus*, *Pelocetus calvertensis* and *Isanacetus laticephalus* the anterior border of the parietal is exposed on the interorbital region of the frontal that, thus, narrows. In Balaenidae, also, the parietal is partially exposed onto the interorbital region of the frontal (Bisconti, 2002).
23. Posterior process of periotic: 0, short; 1, long to very long. Basilosaurinae, Odontoceti (not included in the present study) and Eomysticetidae have short posterior process of the periotic; the other mysticetes have long to very long posterior processes.
24. Supraorbital process of frontal: 0, horizontal (same height as interorbital region); 1, gently descending; 2, horizontal (abruptly depressed from infraorbital region).
25. Median keel on palate: 0, absent; 1, present.
26. Mandibular fossa (*sensu* Fraser & Purves, 1960): 0, wide; 1, small.
27. Fossa for malleus on petrosal: 0, fully developed; 1, poorly developed or absent.
28. Fusion of posterior process of petrosal and posterior process of tympanic bulla: 0, no; 1, yes.
29. Fusion of lateral lip of tympanic bulla with anterior process of petrosal: 0, no; 1, yes.
30. Posterior wall of tympanic bulla: 0, convex; 1, bilobated; 2, keeled; 3, flat.
31. Dorsoventral fissure in posterior wall of tympanic bulla: 0, present; 1, absent.
32. Coronoid process of dentary: 0, high; 1, low (at level of dorsal surface of condyle or lower).
33. Rostrum in lateral view: 0, mainly straight; 1, slightly arched; 2, strongly arched.
34. Parietal exposure on the dorsal wall of the skull: 0, parietal present; 1, parietal absent (located under the supraoccipital); 2, parietal absent (divided into two halves by the interposition of the supraoccipital). The parietal is evident at cranial vertex in archaeocetes, Aetiocetidae, Eomysticetidae, *Parietobalaena palmeri*, *Diorocetus hiatus*, *Pelocetus calvertensis* and *Isanacetus laticephalus*. The parietal is superimposed by the supraoccipital in Balaenidae and Neobalaenidae. The parietal is mainly divided into two halves by the interposition of the supraoccipital in Balaenopteridae, Eschrichtiidae and, possibly, in *Cetotherium*-like mysticetes.
35. Axis of main squamosal development: 0, anteroposterior; 1, dorsoventral. A dorsoventral development of the squamosal is observed in Balaenidae and Neobalaenidae.
36. Glenoid fossa of squamosal: 0, short and concave; 1, short and mainly flat; 2, long and strongly concave.
37. Zygomatic process of squamosal: 0, long and slender; 1, short and stocky; 2, long and crescent-shaped.
38. Articular surface of mandibular condyle: 0, posterodorsal; 1, dorsal; 2, posterior.
39. Baleen length: 0, short; 1, middle-sized (eschrichtiids); 2, very long.
40. Manus: 0, small and slender; 1, large and wide; 2, long and narrow.
41. Dorsoventral compression of tympanic bulla: 0, absent (ovoid bulla, high tympanic cavity); 1, present (low bulla, low tympanic cavity).
42. Sigmoid process of tympanic bulla: 0, high; 1, very low.

43. Dorsal border of round window: 0, round; 1, straight.
44. Anterolateral corner of tympanic bulla: 0, not evident; 1, abruptly rounded and short; 2, gently rounded and long; 3, squared; 4, strongly rounded and long.
45. Location of pterygoid: 0, anterior; 1, close to the posterior border of the skull.
46. Pterygoid partially covered by palatines: 0, no; 1, yes.
47. Ventral lamina of pterygoid: 0, absent; 1, present.
48. Cervical vertebrae: 0, free; 1, fused.
49. Mylohyoidal sulcus on ventromedial surface of dentary: 0, absent; 1, present.
50. Anterior torsion in dentary: 0, absent or slight; 1, present and strong.
51. Dorsal fin: 0, present; 1, absent.
52. Ventral throat grooves: 0, absent; 1, present.
53. Stylomastoid fossa: 0, short and shallow; 1, long and shallow with posterior tubercle; 2, short and deep as a notch with floor; 3, short and deep without floor but with roof; 4, long and shallow with roof.
54. Stylomastoid fossa: 0, not prolonged on the posterior process of petrosal; 1, prolonged.
55. Lateral projection of anterior process of petrosal: 0, absent; 1, long and triangular.
56. Skull length about one-third total body length: 0, no, skull shorter; 1, yes.
57. Skull deep: 0, no, skull slender; 1, yes.
58. Dorsolateral borders of maxilla: 0, transversely compressed; 1, wide and flat.
59. Internal opening of the facial canal small and tubular: 0, no; 1, yes.
60. Infundibulum: 0, absent; 1, complete; 2, incomplete.
61. Large foramen transversarium in axis: 0, absent, a small foramen is present; 1, absent at all; 2, present.
62. Lateral borders of supraoccipital: 0, continuously convex; 1, sigmoid convexity; 2, continuously concave; 3, straight.
63. Anterior tip of supraoccipital: 0, round; 1, narrow and squared; 2, pointed; 3, narrow and round; 4, wide and round; 5, wide and squared.
64. Postcoronoid crest and postcoronoid fossa in dentary: 0, absent; 1, present and wide; 2, present but highly reduced.
65. Internal opening of facial canal coalescent into internal acoustic meatus during late ontogeny: 0, yes; 1, no.
66. Superior process of petrosal: 0, high; 1, low.
67. Base of rostrum: 0, wide (lateral process of maxilla short); 1, narrow (lateral process long).
68. Proportions of scapula: 0, high and very short; 1, high and short; 2, high and very long.
69. Squamosal cleft: 0, absent; 1, present.
70. Number of digits in forelimb: 0, five; 1, four.
71. Interorbital region of frontal: 0, wide; 1, narrowed anteroposteriorly; 2, reduced to a subtle sheet posterior to the caudal tip of the ascending process of the maxilla.
72. Posteromedial elements of rostrum strongly indented: 0, no; 1, yes.
73. Caudal tip of ascending process of maxilla posterior to mid-orbit: 0, no; 1, yes.
74. Exposure of interparietal on the dorsal wall of the skull: 0, absent; 1, small; 2, large.
75. Dorsal surface of petrosal posterior to the anterior process: 0, strongly raised; 1, not raised.
76. Position of posterolateral corner of exoccipital relative to postglenoid process of squamosal: 0, far and medial; 1, far and posterior; 2, close and medial.
77. Lateral and medial borders of ascending process of maxilla: 0, parallel; 1, divergent; 2, strongly divergent.
78. Anterior tip of zygomatic process of squamosal: 0, anterior to anterior border of supraoccipital; 1, posterior.
79. Temporal crest of parietal in front of supraoccipital: 0, present and forming a sagittal crest; 1, absent; 2, present and forming two opposite concavities on both sides of interparietal.
80. Antorbital notch on lateral process of maxilla: 0, absent; 1, present.
81. Posterior tip of ascending process of maxilla: 0, pointed; 1, rounded; 2, squared.
82. Temporal crest lateral to supraoccipital: 0, not covering the lateral wall of braincase in dorsal view; 1, overhanging and covering the lateral wall.
83. Position of posterior apex of the lambdoid crest: 0, at level of occipital condyles; 1, posterior to the condyles; 2, anterior to the condyles.
84. Angular process of dentary: 0, high and squared, pterygoid groove absent; 1, low and squared, pterygoid groove absent; 2, low and round, pterygoid groove absent; 3, very low and squared, pterygoid groove present.
85. Lateral and medial borders of anterior process of petrosal: 0, process absent; 1, externally convex; 2, broadly linear; 3, converging anteriorly and giving the process a general triangular shape. In this character only the relative shape of the borders of the anterior process are taken into account. The shape of the end of the process is treated in the next character.
86. Rostral end of anterior process of petrosal: 0, wide (squared or gently rounded); 1, narrow; 2, pointed.

87. Dorsomedial border of tympanic cavity: 0, sharply depressed from posterior to anterior; 1, not depressed.

88. Lateromedial diameter of promontorium: 0, short; 1, long.

89. Groove under the internal acoustic meatus: 0, absent; 1, present.

90. Ascending temporal crest on supraorbital process of the frontal: 0, at the posterodorsal edge of the process; 1, at middle of the process; 2, moved on the anterior border of the process. See comments to characters 3 and 19.

91. Anterolateral portion of zygomatic process of squamosal: 0, parallel to long axis of the skull; 1, slightly divergent; 2, strongly divergent.

92. Round window confluent into perilymphatic foramen: 0, no; 1, yes.

93. Anterior tip of zygomatic process of squamosal: 0, posterior to postorbital corner of supraorbital process of frontal; 1, very close; 2, under the postorbital corner.

94. Ventral border of dentary: 0, transversely round; 1, crest-like.

95. Dorsal border and ventral border of dentary parallel anterior to coronoid crest: 0, yes; 1, no (dorsal border depressed); 2, no (dorsal border has complex profile).

96. Proportions of the forelimb: 0, humerus longer than radius and ulna; 1, humerus slightly shorter than radius and ulna; 2, humerus much shorter than radius and ulna.

97. Coracoid process of scapula: 0, present; 1, absent.

98. Acromial process of scapula: 0, present; 1, absent.

99. Posteromedial corner of anterior process of petrosal reaches the anteromedial corner of promontorium in dorsal view: 0, yes; 1, no.

100. Anterior border of nasal: 0, straight; 1, notched.

101. Posteromedial corner of anterior process of petrosal: 0, not evident; 1, evident but small and triangular; 2, strongly evident, robust and projecting medially.

102. Lateral border of anterior process of petrosal forming a strong emergence posterior to the lateral projection: 0, absent; 1, present and small; 2, present and robust.

103. Lateral border of anterior process of petrosal: 0, straight or slightly convex; 1, concave.

104. Perilymphatic foramen opens into a cavity: 0, cavity small; 1, cavity large.

105. Groove for facial nerve prolonged under the posterior process: 0, no; 1, yes, it forms a deep groove under the process; 2, yes, the route is bounded by a robust lamina; 3, yes, the route is bounded by a subtle lamina.

106. Anterior expansion of premaxilla: 0, absent; 1, present.

107. Lateral border of maxilla anterior to lateral process (when present): 0, straight; 1, continuously convex; 2, sharp corner evident in posterior portion of maxilla that divides the bone into a short posterior part (straight border parallel to long axis of the skull) and a long anterior part (straight border sharply converging toward long axis of the skull).

108. Posterior border of supraorbital process of frontal: 0, directed transversely; 1, directed anteriorly; 2, directed posteriorly.

109. Postorbital corner of supraorbital process of frontal projected posteriorly: 0, no; 1, yes.

110. Anterior border of supraorbital process of frontal: 0, directed transversely; 1, directed anteriorly; 2, directed posteriorly.

111. Nasofrontal suture: 0, anterior to the interorbital region of frontal; 1, located well into the interorbital region of frontal; 2, obliterating interorbital region of frontal.

112. Anterior border of nasal in dorsal view: 0, in the anterior half of the rostrum; 1, in the posterior half of the rostrum; 2, very close to the base of rostrum; 3, located well into the interorbital region of frontal.

113. Contacts of alisphenoid in temporal fossa: 0, alisphenoid comprised between squamosal, parietal and palatine; 1, no alisphenoid exposed in temporal fossa; 2, alisphenoid comprised between squamosal, parietal and pterygoid; 3, alisphenoid comprised between squamosal and pterygoid; 4, alisphenoid comprised between parietal and pterygoid.

114. Alisphenoid exposure in temporal fossa: 0, large (alisphenoid nearly squared); 1, small (alisphenoid dorsoventrally compressed).

115. Contact of alisphenoid with squamosal: 0, linear; 1, pointed.

116. Relationships of pterygoid and squamosal: 0, pterygoid does not appear in temporal fossa; 1, anterolateral diameter of pterygoid not narrowed by the interposition of the falciform process of squamosal; 2, anterolateral diameter of pterygoid narrowed dorsal to hamular process due to an anteroventral expansion of falciform process of squamosal; 3, pterygoid subdivided into two distinct halves by the interposition of the falciform process of squamosal.

117. Position of foramen 'pseudo-ovale': 0, foramen comprised within pterygoid; 1, foramen comprised between squamosal and pterygoid;

2, foramen comprised within squamosal, contact with pterygoid (when present) by a suture.

118. Optic tube location: 0, under the supraorbital process of frontal; 1, slightly in front of posterior border of supraorbital process of frontal.

119. Optic tube: 0, ventrally open; 1, ventrally closed by a lamina from the anteroventral surface of the supraorbital process of the frontal.

120. Postglenoid process of squamosal: 0, slightly lower than ventral surface of zygomatic process of squamosal; 1, same level as zygomatic process of squamosal; 2, markedly lower than zygomatic process.

121. Coronoid crest: 0, long; 1, short.

122. Medial surface of superior process of petrosal: 0, flat; 1, convex; 2, concave.

123. Dorsolateral and ventromedial surfaces of anterior process of petrosal parallel: 0, no; 1, yes.

124. Dorsolateral surface of anterior process of petrosal oblique: 0, yes; 1, no.

125. If convex, medial surface of superior process: 0, crest-like; 1, round; 2, complex.

126. Intertemporal constriction: 0, narrow and long; 1, wide and long; 2, wide and short; 3, narrow and short.

127. Anterior process 'blade-like': 0, no; 1, yes.

128. Protuberance present on premaxilla at anterolateral corner of nasal bone: 0, no; 1, yes.

129. Elongate notch present in posterior border of palatine at posterior end of palate: 0, no; 1, yes.

130. Lateral process of maxilla and supraorbital process of frontal forms a right angle in lateral view: 0, no, the lateral process is prolonged posteriorly and the angle is obtuse; 1, yes.

131. Ascending temporal crest developed distally over the supraorbital process of frontal: 0, no; 1, yes.

132. Ascending temporal crest high and sharp: 0, yes; 1, not.

133. Position of glenoid fossa of the squamosal: 0, posterior to orbit; 1, under the orbit.

134. Lateral squamosal crest projecting anteriorly: 0, no; 1, yes.

135. Roof of stylomastoid fossa: 0, absent; 1, poorly developed; 2, developed as a strong and long structure whose border is round.

136. Floor of stylomastoid fossa: 0, absent; 1, present and flat; 2, present and enveloping ventrally and posteriorly the fossa.

137. Round window dorsoventrally compressed: 0, no; 1, yes.

138. Position of coronal suture: 0, anterior to the anterior border of the supraoccipital; 1, posterior.

139. Curvature of premaxilla: 0, no curvature; 1, regular curvature; 2, irregular curvature. In *Balaenula astensis* and *Eubalaena* the anterior 25% of the premaxilla is directed ventrally interrupting the regular curvature of the rostrum in that region.

140. Curvature of the dorsal surface of the skull: 0, skull mainly straight; 1, regular curvature; 2, irregular curvature. A regular curvature is observed in *Balaena* and *Balaenella*. Irregular curvature is present in *Eubalaena* and *Balaenula*.

141. Distal portion of the infraorbital plate of the maxilla: 0, present; 1, absent.

142. Orientation of the nasals and the proximal rostrum: 0, horizontal; 1, upward.

143. Relief on the parietal squama: 0, absent; 1, present.

144. Spreading of the anterolateral portion of the parietal onto the emergence of the supraorbital process of the frontal: 0, absent; 1, present. The spreading of the parietal onto the emergence of the supraorbital process of the frontal is observed in the genera *Balaenula* and *Eubalaena* among the Balaenidae.

145. Dome on the supraoccipital: 0, absent; 1, present.

146. Posterior outline of the exoccipital in lateral view: 0, squared; 1, round.

147. Height of the ventral surface of the exoccipital: 0, lower than the orbit; 1, at the level of the orbit; 2, higher than the orbit.

148. Groove for the tensor tympanic muscle: 0, present; 1, absent.

149. Dorsoventral groove medial to the zygomatic process of the squamosal: 0, absent; 1, present.

150. Hamular process of pterygoid: 0, undefined; 1, projecting posteriorly; 2, projecting medially.

151. Development of ascending temporal crest: 0, mainly straight; 1, distal half abruptly projecting posterolaterally.

152. Supraorbital process of frontal: 0, very short; 1, short; 2, long.

153. Posterior side of tympanic bulla: 0, transverse crest-like posterior edge present; 1, straight surface.

154. Tympanic cavity: 0, a single cavity; 1, cavity divided into two halves the anterior of which is separated by the posterior one through a crest-like formation.

155. Supraoccipital breadth: 0, supraoccipital strictly compressed transversely at the level of the posterior apex of the lambdoidal crest (the crest projects posteriorly and medially); 1, supraoccipital not compressed (the crest projects posteriorly and laterally); 2, supraoccipital compressed at the level of the posterior apex of the lambdoidal crest (the crest projects only posteriorly).

156. Supraoccipital length in dorsal view: 0, short length compared with maximum breadth;

1, supraoccipital very long and narrow when compared with the maximum breadth (character observed only in *Eomysticetus* and *Cetotheriopsis*); 2, supraoccipital long but not narrow.

157. Dorsal surface of supraoccipital: 0, strongly concave; 1, flat; 2, anteriorly convex and posteriorly concave; 3, mainly convex.
158. Lateral squamosal crest on the zygomatic process of the squamosal: 0, absent; 1, present.
159. Mandibular foramen: 0, wide; 1, small.
160. Mandibular foramen: 0, round; 1, triangular.

161. Position of maximum rising of the dorsal surface of the petrosal relative to the pars cochlearis: 0, over the pars cochlearis; 1, anterior to the pars cochlearis.
162. Secondary squamosal fossa: 0, absent; 1, present.
163. Anterior process of parietal squama: 0, more posterior than posterior border of ascending process of the maxilla; 1, more anterior.
164. Intertemporal region distinctly depressed anteriorly to the anterior border of the supraoccipital: 0, yes; 1, no.
165. Lacrimal exposed dorsally: 0, no; 1, yes.

TAXON × CHARACTER MATRIX

Character states: numbers refer to character states described in the above character list; ? refers to characters impossible to score due to incomplete or null preservation; – means that the character is not found in the taxon.

Protocetus atavus
000000000000??00000000-000000000000000-?0000000000??00-?000-?0000--?0?00-0-0-000-0000-000-000????-
00--?-?0000-000000-000?????0-00---0-??000--000000000-0000000???0-0?

Georgiacetus vogtlensis
0000000000000000000000-000000000000000-000000000000??00-0000-00000--00000-0-0-000-0000-000-0000000-
00--0-00000-000000-0000????0-00---0-??000--000000000-000000000?0-00

Zygorhiza kochii
1111100000000000000000000000100000001-00000000000??00-0000-000000-000000000001010000-
00000000000-000-0-00000-000000-000000000-00-000-00000--0100000000000100000001001

Chonecetus goedertorum
111111111?11??0?0000000200?00100000020-?0000000000?????01?0?0200?0?0000000?000
101000??0??00000000?00???0011010110000?0020????1011-000-???00—00001000000 0?1200???0001

Aetiocetus polydentatus
111111111?11??0?0000000200?00100000020-
?0000000000?????01?0?0200?0?000000?000101000??0??00000000?00???0011010110000?0020????1011-000-
???00--000010000000?1200???0000

Eomysticetus whitmorei
111101111?111111111000000000001000002200?0000000000??00000100002000000?00-000-000-
0001000001000000-00000001101011000??011-0100110?-000-02000-?00001000000011100000100?

Balaena mysticetus
1110211111111111111121111111101121111121111111111111011111012001-00110010-002-1-0-1222010111010110-
10000110020202100210011-00102001001012011111110012 000021022311000010

Balaena montalionis
?110?111??11??111111?1?1?????????2111?21????111????????10?2?01?????0?10-0?2-1-0-
12??????11?1?????1????????2?20210021001?????2?01?0101???1?1?110012?0002??2231???0010

Eubalaena glacialis
1110211111111111111121111111101121111121111111111111011111012004-00110010-002-1-0-1222011111010100-
10000210000002100210011-00102001110012011220001102000002 10 12311000010

Balaenula astensis
1110211111111111111111111111101121111112?1111111111??11?11012003-00110?10-012-1-0-1222010111010100-
10000110000002100210011-0010200?11011201122000101100 0021012311000010

Caperea marginata
1110211111111111110110111110112111121111111111100010?00111-003-00121110-012-1-0-112??10110010200-
10000?20020202200100001201-2000-0110111111000101 1100011022301000010

Pelocetus calvertensis
111121111?11??1111111111111110100000020100040000000??200?010112210002101000001110001120001110 10
200-0000011110101241012000100003000-110010000-000001000 0021?22010011000

Parietobalaena palmeri
111121111?11??11111121111111110100000020?0000000000??200?0101?1211002??10000011100011000011101
0???-0000011110101241012000101003000-010010000-0000010000 021?22210001000

Isanacetus laticephalus
111121111?11??111111111111111110100000020?0000000000??200?0101132?000?0?10000011100011200011101 0
???-0000011110101241012000100003000-010010000-000000000?02 1?2201??00001

Diorocetus hiatus
111121111?11??11111111111111110100000020?0003000000??200?0101112?11120?10001011100011310011001 0?0
0-0000011120101241012000111003000-000010000-000001000 0021?22210010000

Cetotherium rathkei
111111111?11??111111111111111110110201120?0003000000?????01?1111???1???21121120211011??00?1001????00
????11201122210120011????2?00-0100???00-0000010?1?011?1201???0110

Mixocetus elysius
111111111?11??111111111111111101102011?0?0003000000????001?1133???1???21121120211011??00?1001????0
0?????120112221012001 1????2?00-0000???00-0000000?11011?1201???0110

Titanocetus sammarinensis
?11111011?11??11111121?110?????10002320?????000000?????01?12001?0?0?2111?200200011?????20?000????0
?????10111122101??011????3?00-1100???00-0000000?0002??220001?0000

Metopocetus durinasus
111111??1??11???11111?1????111????2011?0?000?000000????0?0?01?13?10??1?21121120211011 3100??001????-
00000??1???12221012????11113000-???010000-?00?00?0??????122???10110

Eschrichtius robustus
111111111?1111111111011111111101112011110000200000011 0?0001011310111?11211211002110203101111011010
0101000?2020112221012001-210-2000-110010001-00000?00121 11012211000110

Balaenoptera acutorostrata
11101111111111111011211211111121102022202000020000001300001011152111211211111201002123321 1020021
2001010102002202222102110111 1002000-100011000-000000010102 1012201000110

Balaenoptera physalus
111011111111111110112112111111211020222020000200000014100010111521112112112111120100212332 11020021
200?1101130021022341-11101011002000-100011000-0000000101 021012201000110

Balaenoptera musculus
11111111111111111011211211111121102022202000200000001??0001011152?1021121111201002023321102002
120001?????0111022341-32101011022000-100011000-0000000101021 012201000110

Balaenoptera borealis
1110111111111111101121121111112110202220200002000000130000101115211121121111201002123332 0102012
12000021112002002224 1-21101111002000-100011000-000000010102 1012201000110

Balaenoptera edeni
11101111111111111011211211111121102022202000020000001300001011152111211211111201002123320 1020021
2000021112002002222 1121101111002000-100011000-000000011102 1012201000110

Balaenoptera omurai
1110111111111111101121121111112110202220200020000000 1???001011152??12112111?201002123?????20?2120
0?0?????0010022221121 1011????2000-100011000-000000010102 1012201000110

Megaptera novaeangliae
1110111111111111111211211111121102022202000020000001300001011 13-1112112111
120100112332010220212111110001001202231--21102-10002000-100011000-000000010102 1012201000110

Megaptera hubachi
111111111?1111111011211211?11211020222020002000000???0001?11151?112112111201001123 3201?2202121
10?200??00110222???1110111?0?2000-100011000-000000010102 1012201000110

Megaptera miocaena
111111111??11??111111?1121?11111102022?0?0002000000????0?0101115?111?1?21111201001 12?320102201????0
0?000???1102221--?1102?11002000-10001100?-0000000101 02101220??00110

'Plesiocetus' cortesii
111111111?1111111?11112111111110202220000020000000????001?11121??12??2111?101001113?????22?1?000?
0?????01211222?????10?1????2?00-1000???00-0000000?0?021?122010?0110

MPST 240505

111?111?1?1111111?11211211111211 0202220?0002000000??410001011??1110????1110?0??01??331111??1?1???0?21003111??12?????????11102?00?-????100?0-00??0???????10??1?110????

'Balaenoptera' borealina

111?1???1?11??111?11111?111112110?022?0?0002000000???0001011??111???????0????0????31011??1?2??0?2101??????2??????????1102?0???????1?0??????????0????10?????0????

Parabalaenoptera baulinensis

111011111?11??111011211211?????10202220?0002000000?????01?11310??0?1?2111?201000123?????22?11????0?????01110222????21020????2?00-1000???00-0000000?0?021?122010?0110

MCA 240536

?11011111?11??111111011211?????02021?0?????000?00?????01?1?10???1?1?2111?10010110??????22?100????0????12111223110?101?????2?00-0100??00-0000000?0?01??1220???0110

Eschrichtioides gastaldii

?11111?11?11??11111121?201?110110001110?00?0011000?????01?12230????0?2112?1002?1020????12?100?0??0?????1?1?012???110012????2000-1100???00-0000010?1211??122110?0110